KOH electrochemical modification of fluorinated graphite and its reaction mechanism

Hao Li (376467729lihao@163.com)
Xi'an Research Institute of High-Tech
Xiaojing Yuan
Xi'an Research Institute of High-Tech
Genliang Hou
Xi'an Research Institute of High-Tech
Song Bi
Xi'an Research Institute of High-Tech
Yongzhi Song
Xi'an Research Institute of High-Tech
Xuping Wang
Xi'an Research Institute of High-Tech

Research Article

Keywords: Oxidized fluorinated graphite, KOH modification, Nucleophilic reaction, Electrochemical reaction, Carbon-fluorine bond activation

Posted Date: March 15th, 2022

DOI: https://doi.org/10.21203/rs.3.rs-1415583/v1

Abstract

The KOH electrochemical method and heating method were employed to modify fluorinated graphite to explore the modification mechanism. The chemical composition and microstructure of the products were characterized and analyzed before and after the reaction. As the electrochemical reaction time or heating temperature increased, the carbon-fluorine bond gradually underwent a nucleophilic reaction with KOH according to its activity, promoting the formation of F ions in the residual product and carbon-oxygen bonds in the corresponding oxidized fluorinated graphite (OFG). The electrochemical method with a bottom anode and the heating method are insufficient to allow the isolated carbon-fluorine bond to react, retaining partial carbon-fluorine bonds. When the anode is positioned on the top, electron transfer significantly accelerates the activation of the carbon-fluorine bond, which then reacts completely. According to theoretical simulation calculations, electronegative groups around the carbon-fluorine bond can effectively enhance its reactivity.

1 Introduction

Graphene grafted with fluorine atoms and oxygen-containing groups is known as oxidized fluorinated graphite (OFG). OFG has a partial structure of fluorinated graphene (FG) and graphene oxide (GO) at the same time, and its performance is between them [1]. The properties of OFG, such as hydrophilicity [2], lubricity [3], insulation [4], photoelectric performance [5], can be significantly adjusted by varying its content of F and O.

Owing to its unique performance, OFG is widely used in hydrophobic coatings [6], sensors [7], medicine [8], lithium batteries [9] and many other applications. According to the raw materials, OFG preparation can be roughly divided into two types. One is to use GO as a raw material and use HF, XeF_2 and HPF_6 as fluorinating agents to obtain OFG [10–12]. OFG was synthesized by plasma discharge method in a dielectric barrier (DBD) plasma reactor, taking NF_3 as the F-radical-generating gas, and H_2 catalysed the dissociation of NF_3 [10]. GO was fluorinated by SF_4 to obtain OFG below the decomposition temperature of GO (~ 200 ℃) under the catalysis of HF [11]. OFG was also prepared by fluorinating GO with HPF6, which has a sensitivity of roughly 7 nM for histamine detection [12]. Another approach is to prepare OFG using fluorinated graphite (FGi) as a raw material via oxygen doping [13–15]. Mathkar used the Hummers method to oxidize the FGi of $(CF_{0.25})_n$ and the solution separation method to obtain a high fluorine content OFG with good hydrophobicity and a low fluorine content OFG dispersed in water [15]. The FGi(F/C = 1)/DMF solution was also heated to prepare OFG [14].

In addition, FGi is superposed by FG. Theoretical calculations have suggested that FG is vulnerable to S_N2 nucleophilic attack and can be used as a precursor to other graphene derivatives [16]. FG can be nucleophilically substituted by amines [17] and hydroxyl [18] and reduced by hydrazine [19], KI [20], Zn [21], etc. So FGi could be nucleophilically substituted by hydroxyl to synthesize OFG with hydroxyl. A 180 ℃ molten KOH and NaOH mixture was used to modify FGi, obtaining OFG quantum dots (about 3nm), which have a stable fluorescence and can be applied at different pH [22]. A mixture of NaOH-KOH and FGi

was heated at 250 ℃ for 8 hours, to obtain graphitized carbon particles [23]. However, the high temperature molten alkali makes it difficult to control the fluorine and oxygen content of OFG.

As previously reported, there are two main methods for preparing OFG [10–15]. However, it is still difficult to control the contents and types of fluorine and oxygen. The type of oxygen-containing group can be controlled by modifying FG with OH^-; however, there are still two problems. First, it is difficult to control the oxygen content due to the violent reaction between the molten alkali and FGi, which causes FGi to lose nearly all F elements [22]. Second, the reaction mechanism of this process is unclear [23]. In view of this, KOH heating or electrolysis in an organic solvent was adopted to avoid severe damage to the high-temperature molten alkali on FGi. In addition, the reaction processes and products were studied in detail to elucidate the reaction mechanism.

2 Experimental Section

2.1 Materials preparation

FGi with a fluorine contents of ~ 42 wt%, ~ 60 wt% and ~ 65 wt% was provided by Shanghai CarFluor Ltd. Potassium hydroxide (KOH), methanol (CH_3OH), and ethanol (CH_3CH_2OH) were provided by Sinopharm Chemical Reagent Co., Ltd. Deionized water (> 18MΩ.cm) was used as the rinsing and solvent.

2.2 Synthesis of OFG

Considering that only water and carbon dioxide or carbonate are formed following methanol electrolysis, and no organic products are generated, so methanol was selected as the solvent for electrolysis [24]. Because methanol has a low boiling point, ethanol was used instead of methanol in the heating method.

KOH electrochemical method in methanol: 8 g KOH was dissolved in 60 ml methanol by stirring. 0.5g FGi 65 wt% was added, and the mixture was stirred for 5 min to ensure uniform dispersion. The mixture was poured into a tapered, bottomed vertical glass cylinder with an inner diameter of 25 mm, as showned in Fig. 1. Both the anode and cathode were made of Pt wire. When the anode was at the top, the solution was electrolyzed at 60 V DC for a certain period, during which methanol was continuously added to keep the volume of the solution unchanged. After the final solution was poured into a beaker, it was ultrasonically dispersed for 30 min in water to uniformize it and facilitate stripping. After filtration, the solid was freeze-dried in water for 48 h and then dried at 100 ℃ for 12 h to obtain the final product. Following the previous experimental steps, after electrolysis for 2 h, 5 h and electrolysis until there was no current, the products were recorded as OFG65-1, OFG65-2 and OFG65-3, respectively. When the other experimental condition was the same, except for changing the anode of OFG65-3 to the bottom, OFG65-4 was obtained.

KOH heating method in ethanol: 8 g KOH was dissolved in 60 ml methanol by stirring. 0.5g FGi 65 wt% was added, and the mixture was stirred for 5 min to make uniform dispersion. The solution in the sealed beaker was stirred for 24 h at 20℃, then added to water, freeze-dried for 48 h, and finally dried at 100℃

for 12 h to obtain the final product OFG65-5. The corresponding products at 40℃, 60℃, 80℃ and 100℃ were OFG65-6, OFG65-7, OFG65-8 and OFG65-9 respectively.

The KOH modification of FGi 60 wt% followed a similar procedure. By replacing FGi 65 wt%, which was used in synthesizing OFG65-3 and OFG65-9, with FGi 60 wt% and keeping other experimental condition the same, OFG60-1 and OFG60-2 were obtained, respectively. FGi 42 wt% was modified using the same method as that used for FGi 60 wt% and the corresponding products were OFG60-1 and OFG60-2, respectively.

2.3 Separation and extraction of residual products

The chemical components of OFG and residual products were analyzed in detail to study the reaction mechanism of FGi with different fluorine contents modified by KOH. After OFG was separated by suction filtration, the remaining solution was dried at 140 ℃ for at least 48 h, and the product was recorded as a residual product (RP). Thus, RP65-1 corresponded to the residual product of OFG65-1.

2.4 Characterization

Fourier transform infrared (FT-IR) from 400 cm^{-1} to 4000 cm^{-1} were recorded by using a VERTEX70 spectrometer (Bruker, Germany). X-ray photoelectron spectroscopic (XPS) analysis was performed using an X-ray photoelectron spectrometer (Thermo Fisher Scientific, USA) with a monochromatic Al Kα (1486.6 ev) line. All binding energies were calibrated using 284.6 eV of C 1s. The crystal structure was characterized using an X-ray diffractometer with an excitation source of the Ka line of the Cu target (λ = 0.154nm) (X'Pert PRO, PANalytical, Netherlands). The micromorphology was observed using a VEGA2XMU scanning electron microscope (SEM, TESCAN, Czech Republic), and the products were directly adhered to a conductive carbon belt for gold spraying. The distribution of the elements was measured by an Oxford 7718 (EDS, Oxford, UK) instrument equipped with an SEM. The F ion concentration was determined using ion chromatography (Thermo Fisher, ICS-1000 type, USA).

3 Results And Discussion

FGi with a high fluorine content possesses a large number of carbon-fluorine bonds and few unsaturated carbon-carbon bonds. Owing to the small radius and high electronegativity of F, the carbon-fluorine bond has a high degree of polarization, making it the strongest single bond formed by the carbon atom [25]. Although the C-F bond has a very high bond energy, its polarity is very high, which makes it easy to break [16]. Consequently, F is replaced by nucleophiles, but the selectivity of the nucleophilic substitution reaction remains a great challenge. KOH was utilized to react FGi by controlling the reaction conditions.

3.1 Morphology and chemical composition of OFG

3.1.1 KOH electrolytic method in methanol solution

FGi was electrolyzed in a KOH methanol solution and the effect of FGi modification was studied by controlling the reaction time and other conditions. OFG65-1, OFG65-2, OFG65-3 and OFG65-4 correspond to electrolysis for 2 h and 5 h, respectively, until there is no current and the anode at the bottom until there is no current. Figure 2 illustrates the FT-IR and XPS spectra of OFG under different electrolysis conditions. Compared to FGi 65 wt%, OFG65 exhibits obvious changes, especially OFG65-3 and OFG65-4 under complete electrolysis. In Fig. 2a, the characteristic peak (1345 cm^{-1} and 1190 cm^{-1}) for C-F and - CF_2 gradually disappeared from OFG65-1 to OFG65-4. Figure 2b shows that the F1s peak of OFG65-3 almost disappeared and OFG65-4 weakened, corresponding to the disappearance or weakening of the carbon-fluorine bonds. In addition, oxygen-containing groups (-OH vibration peaks near 3438 cm^{-1} and C-O vibration peaks around 1041 cm^{-1}) begin to appear in the FT-IR spectrum, while the O1s peak of OFG65-3 and OFG65-4 increases prominently and the O auger peak becomes evident, but the C1s peak intensity does not changed significantly in the XPS spectrum. This illustrates that FGi gradually begins a nucleophilic reaction with KOH as the electrolysis time increases. The peak of OFG65-4 near 1568 cm^{-1} may belong to the A_{2u} vibration mode of the graphite phase [26], or it may originate from K_2CO_3 residues generated during the electrolysis of the KOH methanol solution.

Table 1 shows the contents of C, O and F of OFG65 after the KOH electrochemical method. The O content of OFG65 gradually increases with the increase of electrolysis time, whereas the F content decreases. The increase in O content is equivalent to the decrease in fluorine content, indicating that KOH undergoes a nucleophilic reaction with the carbon-fluorine bond, and the OH^-exchange position with F. It is noteworthy that the O contents of OFG65-3 and OFG65-4 are basically consistent, but the F content of OFG65-3 is only 1.74 at%, while that of OFG65-4 is 11.4 at%, indicating that the position of the anode has a great influence. Furthermore, the existence of trace amounts of Na, K and Si result from the reaction of KOH with the glass container. According to Fig. S1 in the Supporting Information, the elemental distribution of OFG65 is uniform after KOH electrochemical modification, especially for F and O.

Table 1
Element content of OFG65 after KOH electrochemical method

Products	C(at%)	O(at%)	F(at%)	others(at%)
FGi 65 wt%	45.1	0.6	54.3	
OFG65-1	44.6	2.3	52.6	Si 0.5
OFG65-2	45.8	2.7	51.5	
OFG65-3	69.7	21.8	1.7	Na 0.4; K 4.4; Si 2.0
OFG65-4	64.5	20.0	11.4	Na 0.5; K 2.5; Si 1.1

High-resolution C1s and F1s spectra of OFG65 after the KOH electrochemical method are shown in Fig. 3 and Fig. 4. Table 2 illustrates the compositions of the different carbon bonds in C1s. The carbon-oxygen bonds gradually increase with electrolysis time, which are mostly C-O bonds (286.5 eV) with no C = O

bond (287.8 eV) and a few possible O-C = O bonds (288.5 eV). C-O is not further oxidized, despite the presence of an electrochemical oxidation potential on the anode. The C-O bond of OFG65 is derived from the nucleophilic reaction between KOH and the C-F bond in graphite fluoride [27]. OFG65-1 and OFG65-2 have a carbon-oxygen bond of about 5%, while OFG65-3 and OFG65-4 have over 24%, indicating that the carbon-fluorine bond happening nucleophilic reaction with KOH increases with time. In the case of OFG65-3 and OFG65-4, when the electrolysis time is sufficient, the anode position results in different F content. OFG65-3 only owns a few C-F covalent bonds (688.4 eV), whereas OFG65-4 has a large number of semi-ionic C-F bonds (687.2 eV) and C-F covalent bonds [28, 29], which indicates that part of the covalent bond is converted into a semi-ionic C-F bond. In addition, the increase in carbon-oxygen bonds is not completely consistent with the decrease in carbon-fluorine bonds, and a large part of carbon-fluorine bonds are converted to carbon-carbon bonds. A likely explanation is that KOH undergoes a nucleophilic reaction with the carbon-fluorine bond, but the condensation reaction of carbon-oxygen bonds reduces the oxygen content and leads to the formation of carbon-carbon bonds.

Table 2
Location, ascription and content of carbon-containing groups of OFG65 after KOH electrochemical method

Products	sp^2 C = C ~ 284.6eV	sp^3 C-C ~ 285.3eV	C-O ~ 286.6eV	CO_3^{2-}/semi-ionic C-F ~ 288.5eV	C-F ~ 289.5eV	π-π*/-CF_2 ~ 291.6eV
FGi 65 wt%	0.8%	0.2%	0.3%		83.8%	14.9%
OFG65-1	3.1%	1.3%	5.0%	0.5%	79.1%	11.0%
OFG65-2	3.5%	6.2%	6.2%	2.7%	71.1%	10.3%
OFG65-3	40.8%	28.5%	24.7%	5.7%	0.3%	
OFG65-4	40.7%	13.4%	28.4%	8.5%	6.5%	2.5%

Figure 5 displays the XRD spectrum of OFG65 obtained by the electrochemical method. FGi 65wt% has two strong diffraction peaks located at ~ 12.7 ° and ~ 40.9 °, respectively, which corresponds to the crystal faces (001) and (100), and the weaker diffraction peaks at ~ 27.2 ° correspond to the crystal faces (002). The (001) diffraction peak belongs to the highly fluorinated hexagonal system, which corresponds to a layer spacing of 6.99 Å; the (002) diffraction peak is associated with the graphite phase; the (100) diffraction peak relates to the length in the C-C plane in the network system [30–32]. A weak (002) diffraction peak in FGi 65 wt% indicates that the fluorination of FGi 65 wt% is incomplete, and there is a small amount of graphite phase. The obvious (002) diffraction peaks of OFG65-1 and OFG65-2 indicate that some graphite phases still exist undergoing short electrolysis, and (001) diffraction peaks change little, demonstrating the preservation of the carbon-fluorine bond. Nevertheless, for OFG65-3, the (001) diffraction peak disappears completely, indicating total destruction of the carbon-fluorine bond, and the weak broad peak at ~ 23.6 ° originates from the graphene structure. In addition to the diffraction peak at

~ 23.6 °, OFG65-4 also owns a weak (001) diffraction peak, indicating that only part of the carbon-fluorine bond structure exists, as highlighted in the above analysis.

The actual photographs and SEM images of OFG65 obtained by the electrochemical method are presented in Fig. 6 and Fig. 7, respectively. Over time, the product's color gradually changes from gray-white to earthy yellow, and then to gray-black from OFG65-1 to OFG65-4, indicating that the carbon-fluorine bond is gradually destroyed and the final color is similar to that of graphene. The micromorphologies of OFG65-1 and OFG65-2 are similar to those of FGi 65 wt%, while OFG65-3 and OFG65-4 are significantly different from the former two, displaying a greater layer spacing and thinner sheet structure. Therefore, introducing -OH during oxygen doping increases the layer spacing and facilitates the peeling of FGi.

Following modification using the KOH electrochemical method, the carbon skeleton is grafted with more hydroxyl groups and fewer carbonyl and carboxyl groups. The reason lies in the nucleophilic reaction occurring between KOH and FGi 65 wt%, in which OH^- replaces the F atom. An increased electrolysis time can promote the nucleophilic reaction, and the C-O bond content increases proportionally. In long-term electrolysis, the positions of the anode and cathode have a great influence on the F content. The O and F contents are 14.6 at% and 1.7 at% respectively when the anode is on the top, and 15.2 at% and 11.4 at% respectively when it is on the bottom. The oxygen content differs slightly, but the fluorine content differs significantly. The results indicate that KOH does not destroy the carbon-fluorine bond in a short time, but long electrolysis will cause substantial damage to the carbon-fluorine bond, and the anode position will have an important impact on the results.

3.1.2 KOH heating method in ethanol solution

In order to further explore the reaction mechanism between KOH and FGi, besides the electrochemical method, a heating method in KOH ethanol solution is also used for the modification of FGi 65 wt%. The influence of different temperatures is studied, and the corresponding products at 20℃, 40℃, 60℃, 80℃ and 100℃ range from OFG65-5 to OFG65-9.

Figure 8 is the FT-IR and XPS diagram of OFG65 obtained by the heating method in KOH ethanol solution. The presence of -OH (3438 cm^{-1}, 1626 cm^{-1}) and C-O (1041 cm^{-1}) groups indicates that KOH modification is evidently effective. Upon increasing the reaction temperature from OFG65-5 to OFG65-9, the characteristic peaks of the C-F bond (1215 cm^{-1}) and -CF_2 bond (1319 cm^{-1}) gradually weaken until it becomes invisible at 100 ℃, indicating that the higher the temperature, the more complete the destruction of carbon-fluorine bond, namely more O content.

Table 3
Element content of OFG65 after KOH heating method

Products	C(at%)	O(at%)	F(at%)	others(at%)
FGi 65 wt%	45.1	0.6	54.3	
OFG65-5	47.0	2.0	50.1	K 0.2
OFG65-6	46.8	2.5	49.7	K 0.4
OFG65-7	49.8	4.2	43.9	K 1.5
OFG65-8	71.3	17.1	7.1	K 3.9
OFG65-9	72.5	18.4	2.9	K 3.9; N 1.8

Table 3shows the contents of C, O and F. With an increase in temperature, the content of O increases gradually, while the content of F decreases. When the temperature is lower than 60 ℃, there is a small increase in O content, retaining a high fluorine content. Once the temperature exceeds 80 ℃, the F content decreases rapidly, and the O content also increases. However, the increase in O content is far less than the decrease in F content. K originates from the residual KOH. According to the above information, at temperatures over 80 ℃, KOH will react with FGi 65 wt% in large quantities, and the sum of F and O contents is not consistent, indicating that only a part of KOH undergoes nucleophilic reaction with carbon-fluorine bonds. Fig. S2 shows the distribution of elements in the products modified by KOH at different temperatures. The distributions of F and O elements are basically the same as those of C.

Table 4
Location, ascription and content of carbon-containing groups of OFG65 after KOH heating method

Products	sp^2 C = C 284.6eV	sp^3 C-C 285.3eV	C-O 286.6eV	C = O 287.8eV	O-C = O/semi ion C-F ~ 288.7eV	C-F 289.5eV	π-π*/-CF_2 291.6eV	-CF_3 292.6eV
FGi 65 wt%	0.8%	0.2%	0.3%			83.8%	14.9%	
OFG65-5	7.6%	6.4%	5.3%		1.4%	68.5%	10.8%	
OFG65-6	4.2%	10.9%	7.2%		3.1%	59.2%	15.4%	
OFG65-7	27.6%	7.8%	5.6%	3.7%	3.4%	23.4%	28.5%	
OFG65-8	50.3%	23.1%	9.5%	5.1%	3.2%	3.9%	1.7%	3.2%
OFG65-9	50.6%	19.9%	14.0%	5.5%	3.6%	4.1%	1.4%	0.9%

Figure 9 and Fig. 10 show the C1s and F1s peaks of OFG65 obtained by the heating method. Table 4 illustrates the carbon bond compositions in C1s. The carbon-fluorine bond content decreases from OFG65-5 to OFG65-9 with increasing temperature, while the carbon-oxygen bond content increases

gradually, similar to the unsaturated carbon bond content. Therefore, the probability of nucleophilic reactions between KOH and the carbon-fluorine bonds in FGi increases with increasing temperature. The increase in carbon-carbon bonds indicates that not all carbon-fluorine bonds are changed into carbon-oxygen bonds, which may be due to the reduction in carbon-oxygen bonds resulting from the condensation reaction of the geminal diol and vicinal diol. A large number of π-π * bonds (291.7 eV) are formed, and -CF_3 (292.6 eV) appears at 80 ℃, which originates from the fracture and detachment of carbon skeleton, resulting in the formation of -CF_3 and many semi-ionic C-F bonds (288.7 eV). At 100 ℃, the content of carbon-fluorine bonds decreases to 5%. In addition, the dehydration and condensation of glycol may also result in the formation of C = O and O-C = O.

Figure 11 shows the XRD diagram of OFG65 obtained by the heating method. The (001) diffraction peak intensity of ~ 12.8 ° belonging to the highly fluorinated hexagonal system decreases with increasing temperature from OFG65-5 to OFG65-9. The diffraction peaks of ~ 38.8 ° and 56.1 ° belonging to NaF exist at the OFG65-5, OFG65-6 and OFG65-7 due to the residual NaF. Furthermore, (002) diffraction peak of ~ 24.5 ° appears in OFG65-8 and OFG65-9 without (001) diffraction peaks, which indicates that more graphene structures stack together regularly to form stronger (002) diffraction peaks. It corresponds to a layer spacing of 3.62 Å, which is smaller than the normal graphite layer spacing, indicating the possibility of intercalations between the layers. The diffraction peaks around 17.9 ° from OFG65-5 to OFG65-9 come from the oxidized graphene undergoing the oxidation replacement of the carbon-fluorine bond. The corresponding layer spacing is 4.96 Å, which is between graphene and GO.

The actual morphology and SEM images of OFG65 obtained using the heating method are shown in Fig. 12 and Fig. 13, respectively. The gray-black color gradually deepens from OFG65-5 to OFG65-9 and the structure loosens with the increasing temperature. With an increase in temperature, the sheet structure becomes smaller and thinner, and nanoscale fragments appear in the large pieces of OFG65-7, which then gradually disappear. The nanoscale fragments may have been completely separated from the large piece structure and subsequently leak into the filtrate during the filtration process, as can be verified by a later analysis of the filtrate. As a result of the introduction of -OH in the modification process, the layer spacing enlarges and makes it easier for FGi to peel off the thin layer structure. In this process, the carbon skeleton is completely destroyed, causing a smaller sheet diameter.

In the KOH heating method, the less nucleophilic reactions occur below 60 ℃, and more nucleophilic reactions above 80 ℃ will cause -OH replace F. However, in this process, only one part of the carbon-fluorine bond becomes a carbon-oxygen bond, and the other part becomes a carbon-carbon bond. In addition, with the introduction of oxygen-containing groups, the OFG becomes thinner and the sheet diameter decreases. Compared to the previous electrochemical method, the heating method can also modify FGi 65 wt%, but only part of the carbon-oxygen bond is formed when the carbon-fluorine bond content drops sharply; thus, only a low-oxygen OFG is obtained. In general, KOH can realize the oxygen doping modification of FGi 65 wt%, but the introduction of oxygen-containing groups also leads to a sharp decline in the fluorine content, thereby preventing the production of OFG with a high fluorine and oxygen content.

Whether the KOH electrochemical method or heating method is used, with the increase in time or temperature, the oxygen content of OFG will increase gradually. However, the oxygen and fluorine contents of the final products are slightly different. The specific reasons for this will be explored later.

Similar to FGi 65wt%, the reaction products of FGi 60wt% and FGi 42wt% are analyzed in the second part of the supporting information. According to Fig. S3-S14 and Table S1-S4, FGi 60wt% and FGi 42wt% also undergo different degrees of nucleophilic reaction with KOH, but the carbon-oxygen bond content is lower due to the fewer carbon-fluorine bonds.

3.2 Chemical composition of residual products

Figure 14 displays FT-IR and XPS spectra of residual product RP65 obtained by the KOH electrochemical method. When the anode is at the top, RP65-1, RP65-2 and RP65-3 correspond to 2 hours, 5 hours and complete electrolysis, respectively. RP65-4 is the residual product of the bottom anode. The KOH FT-IR characteristic peaks (3200 cm^{-1}, 1377 cm^{-1} and 1448 cm^{-1}) and the K2s XPS characteristic peaks indicate that all the four products contain KOH. The peaks of RP65-3 and RP65-4 at 1588 cm^{-1} may be derived from the generated carbonate. In addition, there are weak C = O and C-O stretching vibration peaks at 1725 cm^{-1} and 1060 cm^{-1}, indicating that there is a small amount of carbon-oxygen bonds. In order to confirm the existing forms of C and F, further analysis of C1s and F1s spectra is needed.

The C1s and F1s peaks of RP65-1, RP65-2, RP65-3 and RP65-4 are shown in Fig. 15 and Fig. 16, respectively. All the products own O-C = O bonds and no carbon-fluorine bonds, and there are C-O and C = O bonds in some products, indicating that no OFG exists in the RP65, so the C element should exist as GO. This part of the GO also originates from the oxidation fracture of FGi with a high graphite phase content. F1s contains fluorine ion bond peaks (684.8 eV) and the fully electrolyzed RP65-3 and RP65-4 also own the hydrated fluorine ion peaks (682.9 eV), which exist essentially in the form of F ions. The F ion bond originates from the breakdown of the C-F covalent bond in FGi under the nucleophilic influence of KOH, and the F ion cannot form the fluorosilicate in a strong alkaline environment, so there is no fluorosilicate. The strength of the F1s peak increases significantly with increasing reaction time, indicating that the amount of F ions increases.

Figure 17 displays the FT-IR and XPS diagram of RP65 obtained by the KOH heating method. RP65-5, RP65-6, RP65-7, RP65-8 and RP65-9 are the residual products of 20 ℃, 40 ℃, 60 ℃, 80 ℃ and 100 ℃, respectively. Similar to the electrochemical method, all the RP65 own KOH characteristic peaks (3200 cm^{-1}, 1377 cm^{-1} and 1448 cm^{-1}), weak C = O and C-O peaks (1725 cm^{-1} and 1060 cm^{-1}). At different temperatures, the FT-IR spectrum of the remaining products shows no significant differences, mainly the characteristic peaks of KOH. The XPS spectrum of RP65 mainly contains O, C, K and a small amount of F. The peak of F1s at 20 ℃ and 40 ℃ is significantly weaker than that above 60 ℃, but the difference of F1s above 60 ℃ was not significant. At 20 ℃ and 40 ℃, the F content is below 2 at%, whereas above 60 ℃, the F content is over 4 at%, which indicates that the increasing temperature could improve the modification effect.

The C1s and F1s peaks of RP65 obtained by the KOH heating method are shown in Fig. 18 and Fig. 19, respectively. Similar to the electrochemical method, the existence of a carbon-oxygen bond and no carbon-fluorine bond in all filtrates indicates that C exists in the form of GO. All RP65 own hydrated F ion bonds (683.0 eV), and F ion bonds (684.8 eV) exists in RP65-8 and RP65-9 at higher reaction temperatures. Below 60 ℃, the peak strength of hydrated F ions increases gradually, while it is not obvious at a temperature above 60 ℃. The former KOH electrochemical method can only form an F ion bond when the time is sufficient, showing that the hydration ion is easier to form when the F ion content is low, and the drying at 140 ℃ for 48 h is not enough to remove KF crystal water. The strength of F1s increased significantly with an increase in the reaction temperature, indicating an increase in the content of the F ions.

Like FGi 65 wt%, the content of fluorine ions in the remaining products of FGi 60 wt% and FGi 65 wt% is also very low, as displayed in the supporting information. All the remaining products of FGi modified by KOH contain K_2CO_3 and F ions. The former originates from the reaction between CO_2 and KOH, and the latter is due to the nucleophilic reaction between KOH and the carbon-fluorine bond. As the electrochemical reaction time or the heating temperature increases, the F ion content in the residual product increases, while the fluorine content in the corresponding OFG is gradually decreased.

3.3 Reaction mechanism

Table 5 shows the proportion of carbon-carbon bonds (sp^2 C = C/sp^3 C-C), carbon-oxygen bonds (C-O/C = O/O-C = O), and carbon-fluorine bonds (semi-ion C-F, C-F, -CF_2) in OFG65. OFG65-1 to OFG65-4 are modified by the KOH electrochemical method. With the increase in time from OFG65-1 to OFG65-3, carbon-oxygen bonds increase gradually, but carbon-fluorine bonds almost entirely disappear. The position of the anode makes the carbon-fluorine bond content of OFG65-4 significantly higher than that of OFG65-3. OFG65-5 to OFG65-9 are modified by the KOH heating method. The carbon-oxygen bond content decreases obviously with decreasing temperature, and the rangeability is not consistent with that of carbon-fluorine bonds, that is, not all carbon-fluorine bonds are converted to carbon-oxygen bonds. According to the previous analysis, the increase in unsaturated carbon-carbon bonds also indicates that some of the carbon-fluorine bonds become carbon-carbon bonds after destruction. The F ion bonds in the remaining products of KOH modification indicate that the carbon-fluorine covalent bond of FGi 65 wt% has been destroyed. Table 6shows the F ion content in RP65, as determined by ion chromatography and the F concentration in OFG65, as determined by XPS. With an increase in electrolysis time or temperature, the number of F ions increase obviously. Considering the experimental measurement error, the F ion content of RP65 and the F content of OFG65 are basically consistent with the original F element content of FGi 65 wt%, indicating that no other fluorine-containing substances are generated.

Table 5
Different carbon bond ratios in C1s of OFG65

Products	C C bond	C O bond	C F bond	Products	C C bond	C O bond	C F bond
FGi 65 wt%	1.0%	0.3%	98.7%	OFG65-5	14.0%	6.7%	79.3%
OFG65-1	4.4%	5.0%	90.1%	OFG65-6	15.1%	10.3%	68.0%
OFG65-2	9.7%	6.2%	81.4%	OFG65-7	35.4%	12.7%	27.4%
OFG65-3	69.3%	24.7%	0.3%	OFG65-8	73.4%	16.8%	9.8%
OFG65-4	54.1%	28.4%	7.4%	OFG65-9	70.5%	21.9%	7.6%

Table 6
F content of all products of FGi 65 wt% before and after the modification

Raw material	OFG	F content	RP	F ion content
325 mg	OFG65-1	315 mg	RP65-1	4.4 mg
325 mg	OFG65-2	286.5 mg	RP65-2	40.5 mg
325 mg	OFG65-3	13.8 mg	RP65-3	286.3 mg
325 mg	OFG65-4	52.8 mg	RP65-4	238.0 mg
325 mg	OFG65-5	306 mg	RP65-5	10.6 mg
325 mg	OFG65-6	289 mg	RP65-6	22.6 mg
325 mg	OFG65-7	105 mg	RP65-7	218.4 mg
325 mg	OFG65-8	21.7 mg	RP65-8	299.1 mg
325 mg	OFG65-9	10.6 mg	RP65-9	311.1 mg

Although the bond energy of the C-F bond is extremely high, the high polarity of the C-F bond makes it easy to cleave; therefore, F can be replaced by nucleophiles. Keith suggests that the typical C-F bond is so strong that the nucleophilic reaction is difficult, but the C-F bond energy on the graphene skeleton is weakened, reducing the difficulty of the nucleophilic reactions [33]. FGi was modified by -NH_2 [34–36], -SH [37], Grignard reagent [38], KOH or NaOH [39], respectively, which shows that the carbon-fluorine bond of FGi can indeed produce nucleophilic reactions. Furthermore, there are some differences between the electrochemical and the heating methods.

Generally, the carbon-fluorine bond of organic fluorides is inert. However, under the condition of electroreduction, the fracture of the carbon-fluorine bond connected to the aromatic or alkenyl group is relatively easy because the ability of the π-electron system to accept electrons plays an important role in the subsequent transformation process. The reaction activity and mechanism of the carbon-fluorine bond of trifluoromethyl aromatic hydrocarbons (benzyl fluoride) under the electroreduction condition have been

studied [40], indicating that the double electron reduction of trifluoromethyl aromatic hydrocarbons generates fluorine ions and corresponding carbon anion intermediates that can be captured by electrophilic reagents. According to the above reaction products, the possible reaction mechanism is shown in Fig. 20 and Fig. 21. As shown in Fig. 20, the carbon-fluorine bond connected with aryl and alkenyl groups has high activity, and is the first to undergo nucleophilic reaction with KOH. There are two possible mechanisms for the carbon-fluorine bond reaction connected to the alkenyl group. One is that the hydroxyl attacks the carbon atom directly, resulting in the leaving of the F ion to form alcohol, and the unstable enol is easily converted to carbonyl, as shown in Fig. 20a; the other is that the carbon-carbon double bond undergoes the methanol addition reaction, and the introduction of -OH makes the F ion leave easily while simultaneously accepting an OH^- ion, as shown in Fig. 20b. The carbon-fluorine bond connected to the aryl group can react only in the manner shown in Fig. 20c. There are two possible reaction mechanisms in the presence of electron transfer, one is that the carbon-fluorine bond obtains two electrons by electroreduction, which directly generates fluorine ions and carbon anions, and carbon anions capture hydrogen ions, as shown in Fig. 21a; the second is that a single electron transfers to the F atom, which then becomes the F ion to leave, and then hydroxide is combined with an unstable carbon atom, losing fluorine and releasing an electron, in which electrons act as a catalyst, as shown in Fig. 21b. From the point of view of the products, OFG65 also contains hydrocarbons, and the carbon content of the products increases after the reaction, which proves that there is indeed an addition reaction between methanol and carbon-carbon double bonds.

As shown in Fig. 22, when the carbon-fluorine bond connected with the aryl or alkenyl group reacts completely, the carbon-fluorine bond attached to the carbon atom linked with the alkenyl or aryl group begins the nucleophilic reaction with KOH. Furthermore, nucleophilic reactions may also occur under electron transfer, as shown in Fig. 21. The last reaction is the most inactive alkyl carbon-fluorine bond and the mechanism is similar to the previous one. In addition, the carbon-fluorine bonds in $-CF_2$ and $-CF_3$ undergo nucleophilic substitution, resulting in the formation of geminal diol structures, which are extremely unstable and very easy to dehydrate into aldehydes or ketones, as shown in Fig. 23. Therefore, when $-CF_2$ and $-CF_3$ are completely substituted, they become ketone and carboxyl groups, respectively, explaining the source of carbonyl in the OFG. In addition, the existing carbon-carbon double bond theoretically reacts with the weakly nucleophilic methanol.

As shown in the above mechanism, with the increase in electrolysis time, the carbon-fluorine bond gradually reacts with KOH according to its reactive activity, and then the F atom is replaced. However, according to XPS, not all carbon-fluorine bonds are converted into carbon-oxygen bonds. One reason is that with the increase in time, the carbon-oxygen bond may be partially reduced to a carbon-carbon double bond by the cathode, but this should be a very small percentage. The other reason is that the dehydration polymerization of adjacent hydroxyl groups may occur in the presence of a large number of hydroxyl groups, as shown in Fig. 24a, and the aldol condensation reaction may also occur after the addition of methanol, which forms a carbon-carbon double bond, as shown in Fig. 24b. A large number of carbon-oxygen bonds can also be deoxidized under strong alkalinity [41]: the attack of hydroxyl ions on

carbonyl leads to the fracture of carbon-carbon bonds and the formation of carboxyl groups, and decarboxylation forms the structure shown in the literature, releasing carbon dioxide. This fracture, as well as the oxidation fracture of unsaturated carbon bonds in FGi 65 wt%, also explains the presence of GO fragments in the filtrate.

As shown in Table 5, the carbon-oxygen bond contents of OFG65-3 and OFG65-4 are similar, but the carbon-fluorine bond content is quite different, and the only difference between them is the anode location. This can be explained by the difference in the direction of the ion current and products due to the different anode positions. As shown in Fig. 25, when the anode is at the bottom, it generates CO_2 gas flow adjacent to it, driving FGi to move upward against the flow of OH^- ions. Increasing the contact between the two reactants increases the probability of a nucleophilic reaction. However, OH^- ions react with CO_2 more easily, rather than undergoing a nucleophilic reaction with FGi, so OFG65-4 can maintain a high fluorine content. In the case of an anode at the bottom, CO_2 directly overflows, and the flow of H_2 drives FGi and OH^- ions to move in the same direction; thus, OH^- ions cannot react with CO_2, increasing the probability of nucleophilic reaction. Besides avoiding the reaction of KOH with CO_2, the activation of carbon-fluorine bonds by electron transfer further promotes the nucleophilic reaction between KOH and the isolated saturated carbon-fluorine bonds. These reasons may explain the difference between OFG65-3 and OFG65-4. In addition, OFG65 has no C = O bond and a few possible O-C = O bonds under electrooxidation environment, indicating that 60V DC can't oxidize FGi 65wt%. The reason is that strong alkalis such as NaOH and KOH and their reduction property can suppress the oxidation [42] and the FGi powder moves with the boiling of the solution and the movement of the air flow in it.

The reaction mechanism of KOH heating method is similar to that of the KOH methanol electrochemical method; however, there is no nucleophilic reaction caused by electron transfer. The possible mechanism is shown in Fig. 20, Fig. 22 and Fig. 23. The reaction occurs based on the reaction activity of the carbon-fluorine bond. In addition, full substitution of $-CF_2$ and $-CF_3$ occurs, resulting in the formation of ketone and carboxyl groups, respectively. As shown in Fig. 24, it is deoxidized under strong alkali condition, resulting in the reduction of carbon-oxygen bonds and the fracture of the carbon skeleton. The decrease in temperature results in a decrease of carbon-fluorine bond reaction activity from OFG65-9 to OFG65-5, along with an increase in carbon-fluorine bonds and a decrease in F ions.

According to the previous analysis, KOH can react with the carbon-fluorine bond with stronger activity, and the basic principle is similar, although in different places. The electrochemical method using the bottom anode can destroy most of the carbon-fluorine bonds of FGi 65 wt%, but some are retained. FGi 60 wt% retains more carbon-fluorine bonds under the same conditions, while FGi 42 wt% is in the middle. The same law still exists in the modification of FGi by the KOH ethanol heating method, leaving some carbon-fluorine bonds that can't react with KOH. Only when the anode is on the top using the electrochemical method, these carbon-fluorine bonds can react due to electron transfer activation.

In order to confirm that the dissociation energy of the isolated carbon-fluorine bond is high and difficult to activate to participate in the reaction, the following theoretical simulation calculation is carried out for the

different positions of the carbon-fluorine bond. The methods are as follows: using the DFT method at the level of B3LYP [43, 44] /6-311G (d, p) [45], the whole structure of different carbon-fluorine bonds is optimized. Vibration analysis confirms that there is no virtual frequency at the equilibrium point. The single-point energies of the entire structure, fluorine atom fragments and remaining structures are calculated. The carbon-fluorine bond dissociation energy is obtained by subtracting the single-point energy of the whole structure from the sum of the single-point energies of the two fragments. All the calculations are performed on the Dawning workstation using the Gaussian 09 package [46].

Four different structures are constructed, and their carbon-fluorine bonds are located at different positions, as shown in Fig. 26. Figure 26a shows the isolated carbon-fluorine bond structure. Figure 26b shows the carbon-fluorine bond structure surrounded by other carbon-fluorine bonds, which is similar to the carbon-fluorine bond in FGi with complete fluorination. Figure 26c illustrates the carbon-fluorine bond surrounded by the hydroxy group, assuming that the carbon-fluorine bond undergoes a complete nucleophilic reaction with KOH, and Fig. 26d shows the carbon-fluorine bond surrounded by oxygen-containing groups (hydroxy, carbonyl, carboxyl). After calculation, the dissociation energy of the carbon-fluorine bond in the middle of the four different structures is shown in Table 7. The dissociation energy of the isolated carbon-fluorine bond is much higher than that of the carbon-fluorine bond surrounded by other electronegative groups. When C-O bonds, C = O bonds and O-C = O bonds replace the carbon-fluorine bonds around the carbon-fluorine bonds, the dissociation energy of the carbon-fluorine bond is the lowest. Once the carbon-fluorine bonds are replaced by oxygen-containing groups, the dissociation energy of the carbon-fluorine bonds is reduced, thereby accelerating the reaction of the carbon-fluorine bonds. Due to its highest dissociation energy and lowest reaction activity, the isolated carbon-fluorine bond can only react under the condition of electron catalytic transfer.

Table 7
Dissociation energy of the C-F bond at different positions

C-F bond position	Dissociation energy (kJ/mol)
Isolated C-F bond	489.4
C-F bond surrounding F atoms	437.8
C-F bond surrounding hydroxyl groups	429.1
C-F surrounding oxygen-containing groups	399.3

The residual carbon-fluorine bond of OFG60 is the highest, followed by OFG42, and OFG65 is the least. The reason is that FGi 65 wt% with complete fluorination owns the least isolated carbon-fluorine bond, and the carbon-fluorine bond of FGi 42 wt% with incomplete fluorination is concentrated at the edge and defect, resulting in fewer internal isolated carbon-fluorine bonds, whereas FGi 60 wt%, fluorinated completely at the edge and defect and incompletely in the interior, has more isolated carbon-fluorine bond structures in its internal structure. The isolated carbon-fluorine bond is difficult to participate in the reaction due to its high dissociation energy and weak reaction activity. Electronegative groups can reduce

the dissociation energy of the carbon-fluorine bond and increase its reactivity when they are located around the carbon-fluorine bond.

4 Conclusion

When FGi 65 wt% is modified by KOH, with an increase in the electrochemical time or heating temperature, the F ion content in the residual product of the reaction increases due to the nucleophilic reaction, while the carbon-fluorine bond content in the corresponding OFG is gradually reduced. After complete electrolysis, the oxygen content of the OFG is approximately 15 at%, and the position of the anode greatly affects the fluorine content of the OFG. When the anode is at the bottom, there are still some carbon-fluorine bonds and the F content is 11.4 at%, but at the top, the carbon-fluorine bonds almost completely disappear and the F content is only 1.7 at%. The reason is that CO_2 generated at the anode reacts more easily with KOH than with FGi, thus preventing the nucleophilic reaction between KOH and FGi. Furthermore, the electron transfer greatly promotes the activation of the carbon-fluorine bond, resulting in a complete reaction. FGi undergoes a nucleophilic reaction with KOH according to its carbon-fluorine bond reaction activity, and the F atoms are then replaced. The carbon-fluorine bond connected to the aryl or alkenyl reacts first, followed by the carbon-fluorine bond attached to the carbon atom linked with the alkenyl or aryl, and the isolated carbon-fluorine bond is the last. The reaction mechanism of the KOH heating method is similar except for the promotion of the electron transfer.

OFG60 contains the most residual carbon-fluorine bonds under the same conditions, followed by OFG42, and OFG65 has the least. The reason is that the edges and defects of FGi 60 wt% are completely fluorinated, but the internal fluorination is incomplete, which leads to a more isolated carbon-fluorine bond structure. According to the theoretical simulation calculations, the isolated carbon-fluorine bond owns the highest dissociation energy and the lowest reaction activity, and the introduction of electronegative groups can decrease its dissociation energy and increase its reactivity.

Declarations

Conflicts of interest

The authors have declared that no competing interests exist.

Acknowledgements

This research was supported by the Youth Foundation Program of Xi'an Research Institute of High-Tech (Program No.2020QNJJ009).

Data Availability Statement

All data generated or analysed during this study are included in this published article and its supplementary information files.

References

1. Chen X, Fan K, Liu Y, et al. Recent advances in fluorinated graphene from synthesis to applications: critical review on functional chemistry and structure engineering[J]. Advanced Materials, 2021: 2101665.
2. Zhu W, Wu C, Chang Y, et al. Solvent-free preparation of hydrophilic fluorinated graphene oxide modified with amino-groups[J]. Materials Letters, 2019, 237: 1–4.
3. Fan K, Liu J, Wang X, et al. Towards enhanced tribological performance as water-based lubricant additive: Selective fluorination of graphene oxide at mild temperature[J]. Journal of colloid and interface science, 2018, 531: 138–147.
4. Peiwei Gong, Zhaofeng Wang, Zengjie Fan, et al. Synthesis of chemically controllable and electrically tunable graphene films by simultaneously fluorinating and reducing graphene oxide[J]. Carbon, 2014, 72: 176–184.
5. Chen Xiao, Huang Haohao, Shu Xia, et al. Preparation and properties of a novel graphene fluoroxide/polyimide nanocomposite film with a low dielectric constant[J]. RSC Advances, 2017, 7(4): 1956–1965.
6. Bharathidasan T., Narayanan Tharangattu N., Sathyanaryanan S., et al. Above 170° water contact angle and oleophobicity of fluorinated graphene oxide based transparent polymeric films[J]. Carbon, 2015, 84: 207–213.
7. Kim Yeon-Hoo, Ji Soo-Park, Choi You-Rim, et al. Chemically fluorinated graphene oxide for room temperature ammonia detection at ppb levels[J]. Journal of Materials Chemistry A, 2017, 5(36): 19116–19125.
8. Razaghi M, Ramazani A, Khoobi M, et al. Highly fluorinated graphene oxide nanosheets for anticancer linoleic-curcumin conjugate delivery and T_2-Weighted magnetic resonance imaging: In vitro and in vivo studies[J]. Journal of Drug Delivery Science and Technology, 2020, 60: 101967.
9. Mar M, Dubois M, Guérin K, et al. High energy primary lithium battery using oxidized sub-fluorinated graphite fluorides[J]. Journal of Fluorine Chemistry, 2019, 227: 109369.
10. Sim Y, Surendran S, Cha H, et al. Fluorine-doped graphene oxide prepared by direct plasma treatment for supercapacitor application[J]. Chemical Engineering Journal, 2022, 428: 132086.
11. Yamamoto H, Matsumoto K, Matsuo Y, et al. Deoxofluorination of graphite oxide with sulfur tetrafluoride[J]. Dalton Transactions, 2020, 49(1): 47–56.
12. Mazánek V, Jankovský O, Luxa J, et al. Tuning of fluorine content in graphene: towards large-scale production of stoichiometric fluorographene[J]. Nanoscale, 2015, 7(32): 13646–13655.
13. Guguloth L, Shekar P V R, Channu V S R, et al. Effect of reduced fluorinated graphene oxide as ternary component on synergistically boosting the performance of polymer bulk heterojunction solar cells[J]. Solar Energy, 2021, 225: 259–265.
14. Fan Li, Weili Wei, Die Gao, et al. The adsorption behavior and mechanism of perfluorochemicals on oxidized fluorinated graphene sheets supported on silica[J]. Analytical Methods, 2017, 9(47): 6645–

6652.

15. Mathkar Akshay, Narayanan T. N., Alemany Lawrence B., et al. Synthesis of fluorinated graphene oxide and its amphiphobic properties[J]. Particle &Particle Systems Characterization, 2013, 30(3): 266–272.
16. Dubecký Matúš, Otyepková Eva, Lazar Petr, et al. Reactivity of fluorographene: a facile way toward graphene derivatives[J]. Journal of Physical Chemistry Letters, 2015, 6(8): 1430–1434.
17. Siedle A R, Losovyj Y, Karty J A, et al. C-F bond activation in the solid state: functionalization of carbon through reactions of graphite fluoride with amines[J]. The Journal of Physical Chemistry C, 2021, 125(19): 10326–10333.
18. Kouloumpis A, Chronopoulos D D, Potsi G, et al. One-step synthesis of Janus fluorographene derivatives[J]. Chemistry-A European Journal, 2020, 26(29): 6518–6524.
19. Jeremy T. Robinson, James S. Burgess, Chad E. Junkermeier, et al. Properties of Fluorinated Graphene Films[J]. Nano Letters, 2010, 10(8): 3001–3005.
20. Zboril, Radek, Karlický, et al. Graphene fluoride: A stable stoichiometric graphene derivative and its chemical conversion to graphene[J]. Small, 2010, 6(24): 2885–2891.
21. Liang X, Lao M, Pan D, et al. Facile synthesis and spectroscopic characterization of fluorinated graphene with tunable C/F ratio via Zn reduction[J]. Applied Surface Science, 2017, 400(APR.1):339–346.
22. Peiwei Gong, Zhigang Yang, Wei Hong, et al. To lose is to gain: effective synthesis of water-soluble graphene fluoroxide quantum dots by sacrificing certain fluorine atoms from exfoliated fluorinated graphene[J]. Carbon, 2015, 83: 152–161.
23. Bourlinos Athanasios-B., Georgakilas Vasilios, Zboril Radek, et al. Reaction of graphite fluoride with NaOH–KOH eutectic[J]. Journal of Fluorine Chemistry, 2008, 129(8): 720–724
24. Menia S, Tebibel H, Lassouane F, et al. Hydrogen production by methanol aqueous electrolysis using photovoltaic energy: Algerian potential[J]. International Journal of Hydrogen Energy, 2017, 42(13): 8661–8669.
25. Yang H, Gao H, Angelici RJ. Hydrodefluorination of fluorobenzene and 1,2-difluorobenzene under mild conditions over rhodium pyridylphosphine and bipyridyl complexes tethered on a silica-supported palladium catalyst[J]. Organometallics, 1999, 18(12): 2285–2287.
26. Yan Shijing. Preparation of graphene derivatives and its polyimide nanocomposites [D]. Guangzhou: South China University of Technology, 2014.
27. Mazánek Vlastimil, Libánská Alena, Šturala Dr.-Jiří,et al. Fluorographene modified by Grignard reagents: a broad range of functional nanomaterials[J]. Chemistry-A European Journal, 2017, 23(8): 1956–1964.
28. Lai W., Xu D., Wang X., et al. Characterization of the thermal/thermal oxidative stability of fluorinated graphene with various structures[J]. Physical Chemistry Chemical Physics, 2017, 19(29): 19442–19451.

29. Li B., He T., Wang Z., et al. Chemical reactivity of C-F bonds attached to graphene with diamines depending on their nature and location.[J]. Physical Chemistry Chemical Physics, 2016, 18(26): 505–17495.
30. Sun C., Feng Y., Li Y., et al. Solvothermally exfoliated fluorographene for high performance lithium primary batteries[J]. Nanoscale, 2014, 6(5): 2634–2641.
31. Zhan Liang, Yang Shubin, Wang Yun, et al. Fabrication of fully fluorinated graphene nanosheets towards high-performance lithium storage[J]. Advanced Materials Interfaces, 2014, 1(4): 1–4.
32. Chen Qi, Ji Yan, Zhang Danying, et al. Fabrication of fluorographene nanosheets with high yield and good quality based on supercritical fluid-phase exfoliation[J]. Springer Netherlands, 2016, 18(7): 199.
33. Jr Keith-E.-Whitener, Stine Rory, Robinson Jeremy-T., et al. Graphene as electrophile: reactions of graphene fluoride[J]. Journal of Physical Chemistry C, 2015, 119(19): 10507–10512.
34. Bosch-navarro Concha, Walker Marc, Wilson Neil-R., et al. Covalent modification of exfoliated fluorographite with nitrogen functionalities[J]. Journal of Materials Chemistry C, 2015, 3(29): 7627–7631.
35. Ye Xiangyuan, Ma Limin, Yang Zhigang, et al. Covalent functionalization of fluorinated graphene and subsequent application as water-based lubricant additive[J]. Applied Materials & Interfaces, 2016, 8(11): 7483–7488.
36. Hou K, Gong P, Wang J, et al. Structural and tribological characterization of fluorinated graphene with various fluorine contents prepared by liquid-phase exfoliation[J]. RSC Advances, 2014, 4(100): 56543–56551.
37. Urbanová Veronika, Holá Kateřina, Bourlinos Athanasios-B., et al. Thiofluorographene-hydrophilic graphene derivative with semiconducting and genosensing properties[J]. Advanced Materials, 2015, 27(14): 2305–2310.
38. Chronopoulos Demetrios-D., Bakandritsos Aristides, Lazar Petr, et al. High-yield alkylation and arylation of graphene via grignard reaction with fluorographene[J]. Chemistry of Materials, 2017, 29(3): 926–930.
39. Zhang Guoxin, Zhou Kang, Xu Ruoyu, et al. An alternative pathway to water soluble functionalized graphene from the defluorination of graphite fluoride[J]. Carbon, 2016, 96: 1022–1027.
40. Andrieux CP, Combellas C, Kanoufi F, et al. Dynamics of bond breaking in ion radicals. mechanisms and reactivity in the reductive cleavage of carbon – fluorine bonds of fluoromethylarenes[J]. Journal of the American Chemical Society, 1997, 119(40): 9527–9540.
41. Dimiev AM, Alemany LB, Tour JM. Graphene Oxide. Origin of acidity, its instability in water, and a new dynamic structural model[J]. ACS Nano, 2012, 7(1): 576–588.
42. Alshamkhani Maher-T.,Teong Lee-Keat,Putri Lutfi-Kurnianditia, et al. Effect of graphite exfoliation routes on the properties of exfoliated graphene and its photocatalytic applications[J]. Journal of Environmental Chemical Engineering, 2021, 9(6): 106506.
43. Perdew JP, Wang Y. Accurate and simple density functional for the electronic exchange energy: generalized gradient approximation[J]. Physical Review B, 1989, 33(12): 8800–8802.

44. Lee C, Yang W, Parr RG. Development of the colle-salvetti correlation-energy formula into a functional of the electron density[J]. Physical Review B, 1988, 37(2): 785–789.
45. Ditchfield R, Hehre WJ, Pople JA. Self-consistent molecular-orbital methods. ix. an extended Gaussian-type basis for molecular-orbital studies of organic molecules[J]. Journal of Chemical Physics, 1971, 54(2): 724–728.
46. Gaussian09 RA. 1, Mj Frisch, Gw Trucks, Hb Schlegel, Ge Scuseria, Ma Robb, Jr Cheeseman, G. Scalmani, V. Barone, B. Mennucci, Ga Petersson Et Al., Gaussian[J]. Inc., Wallingford Ct, 2009, 121: 150–166.

Figures

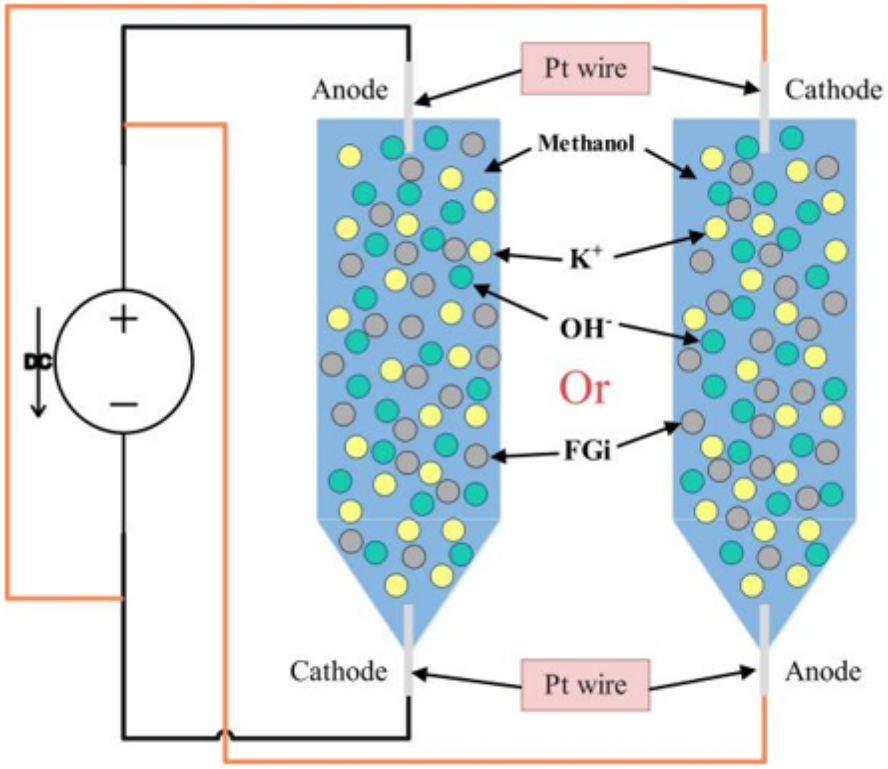

Figure 1

Electrolytic device of KOH methanol solution

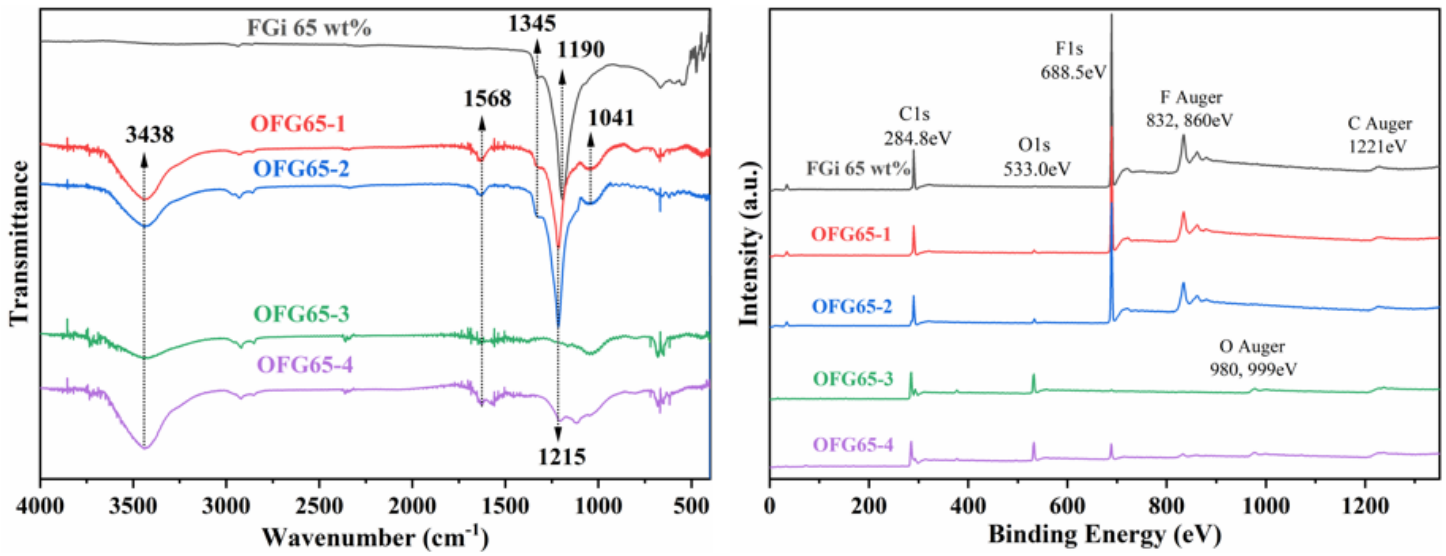

(a) FT-IR spectrum (b) XPS spectrum

Figure 2

(a) FT-IR and (b) XPS spectra of OFG65-1(2h), OFG65-2(5h), OFG65-3(no current) and OFG65-4(bottom anode)

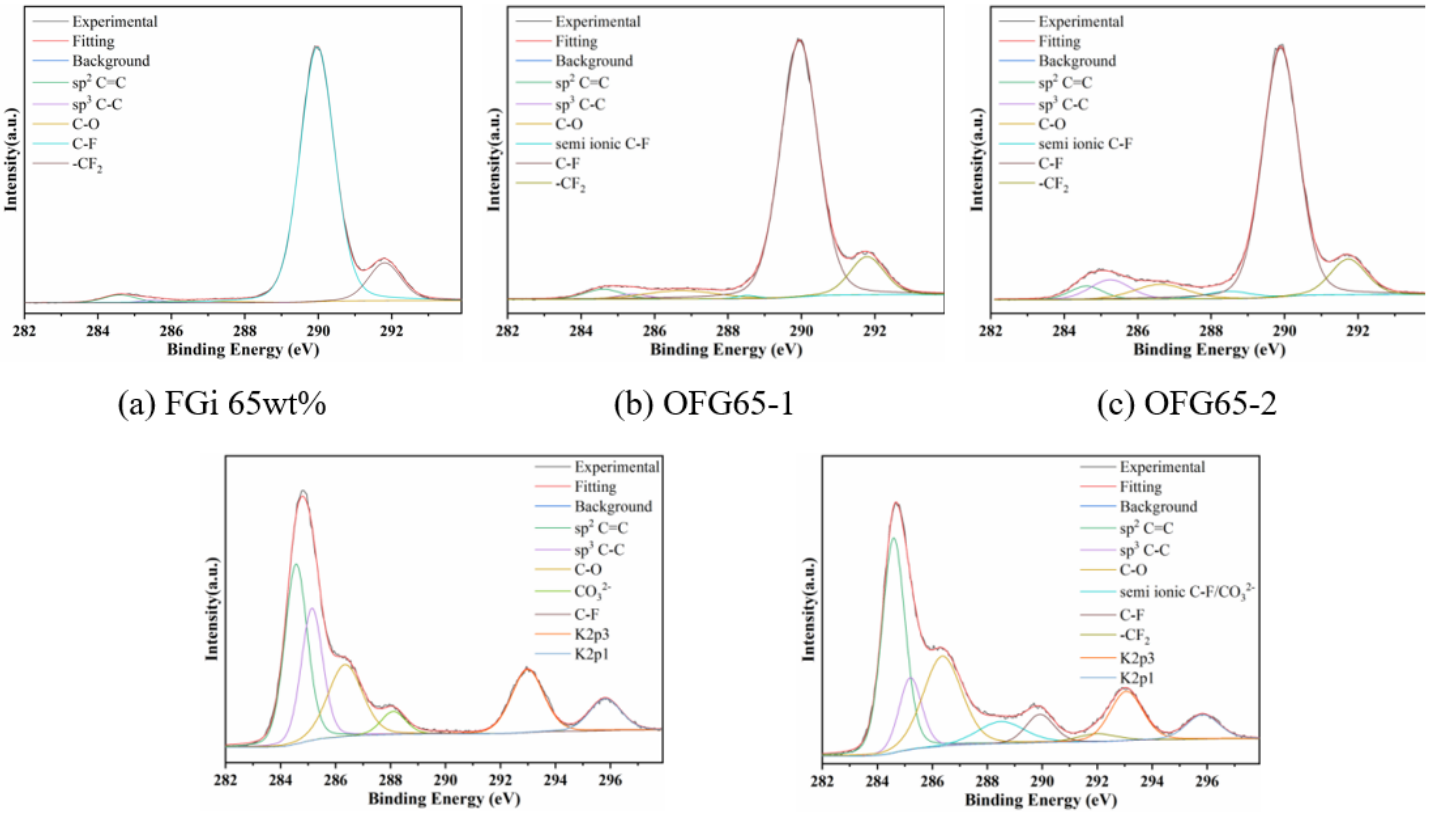

Figure 3

High-resolution C1s spectra of OFG65 after KOH electrochemical method

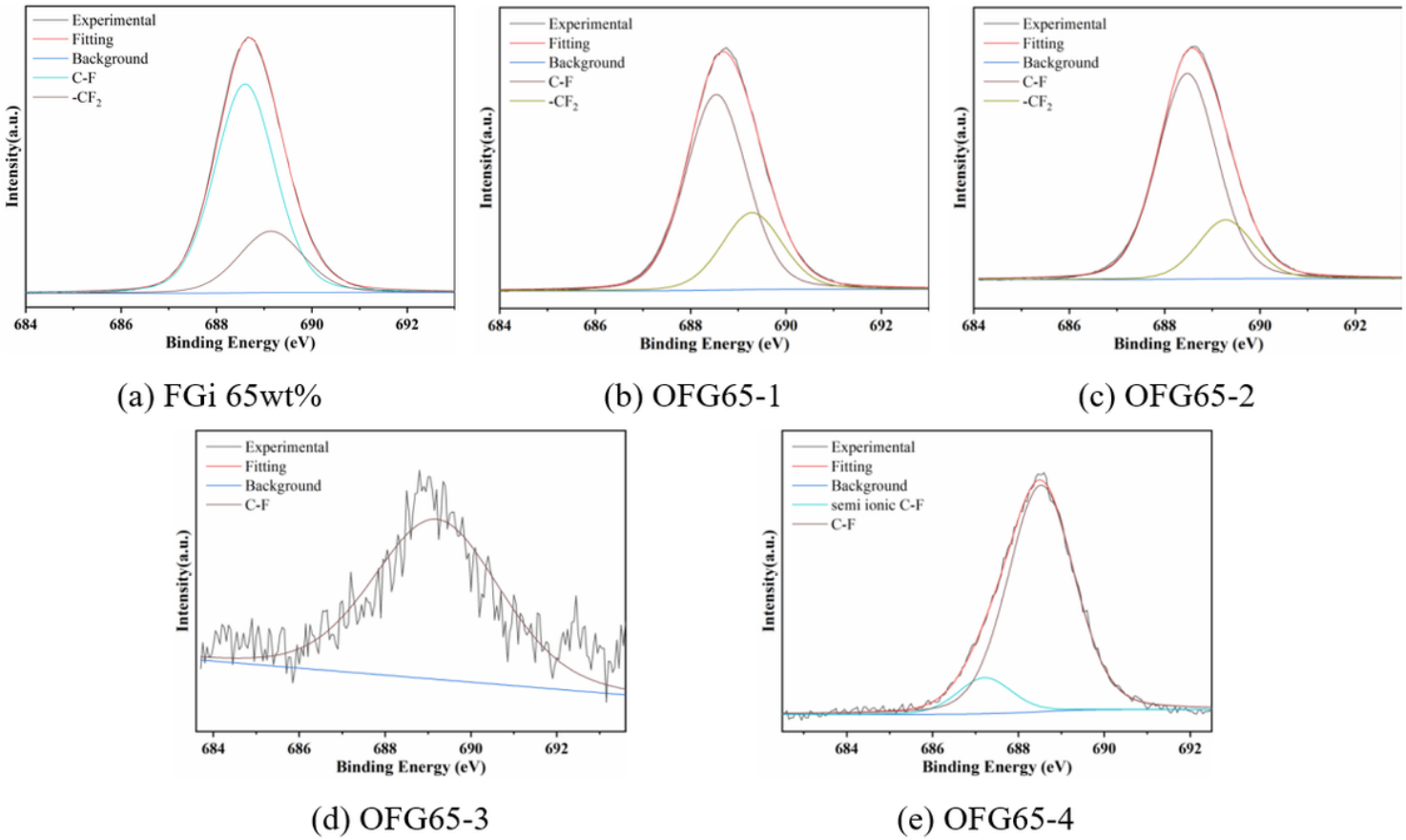

Figure 4

High-resolution F1s spectra of OFG65 after KOH electrochemical method

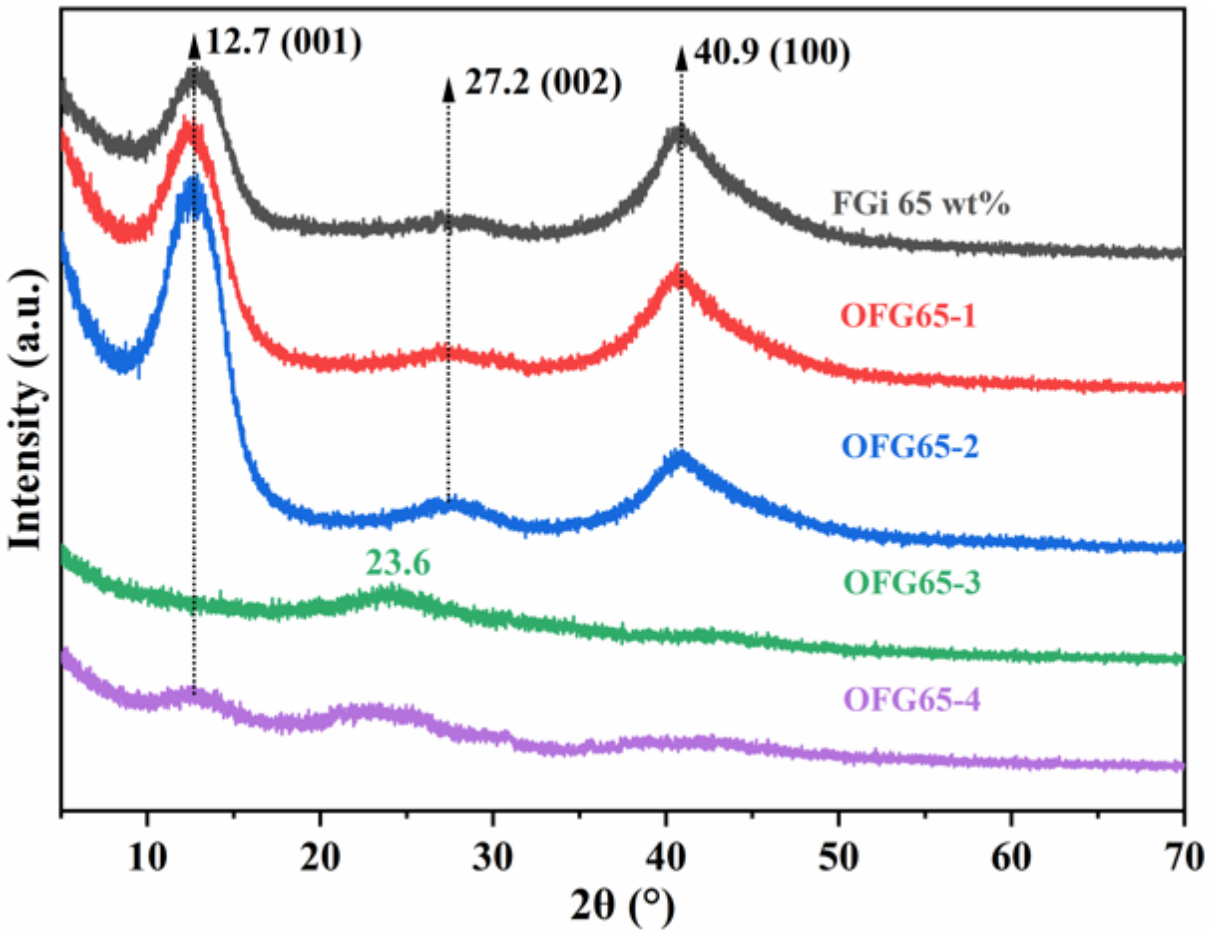

Figure 5

XRD spectrum of OFG65 after KOH electrochemical method

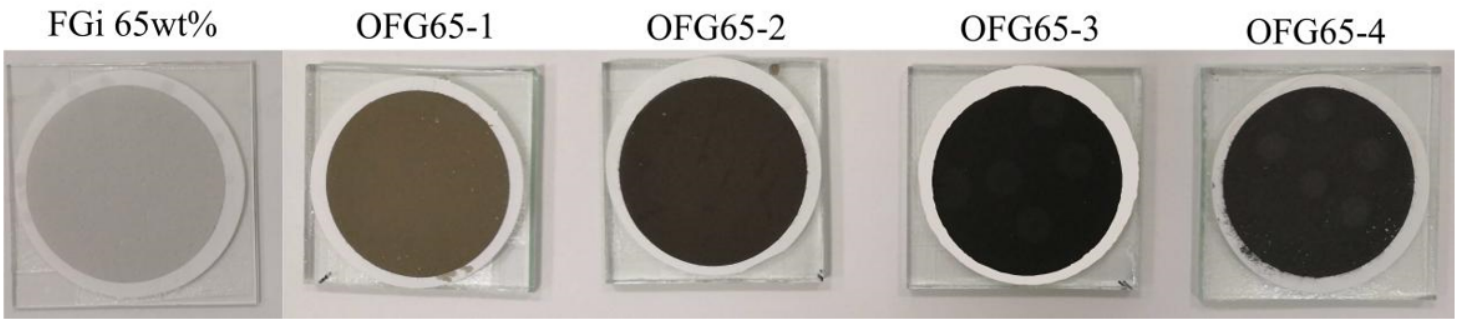

Figure 6

Photos of OFG65 after KOH electrochemical method

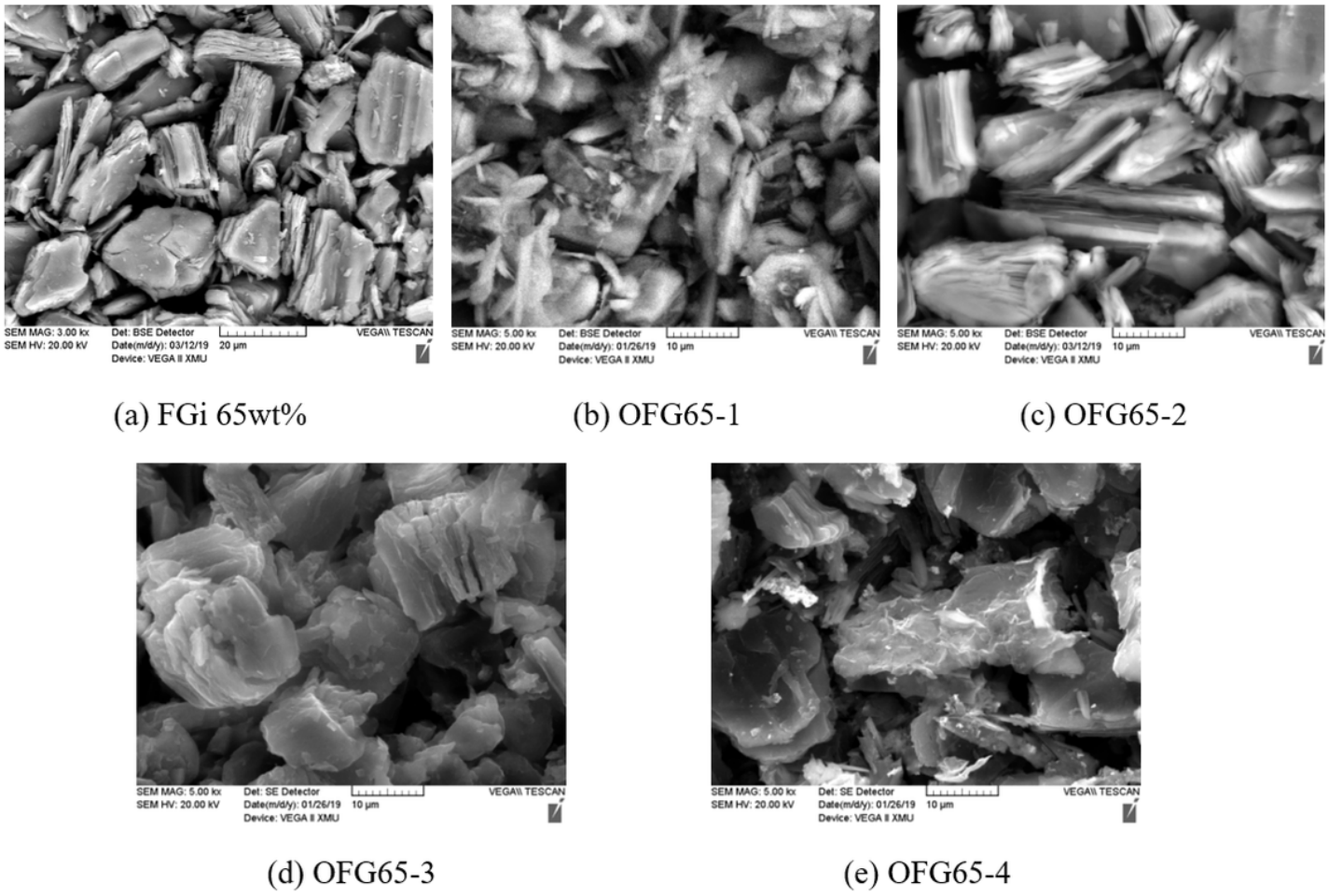

Figure 7

SEM images of OFG65 after KOH electrochemical method

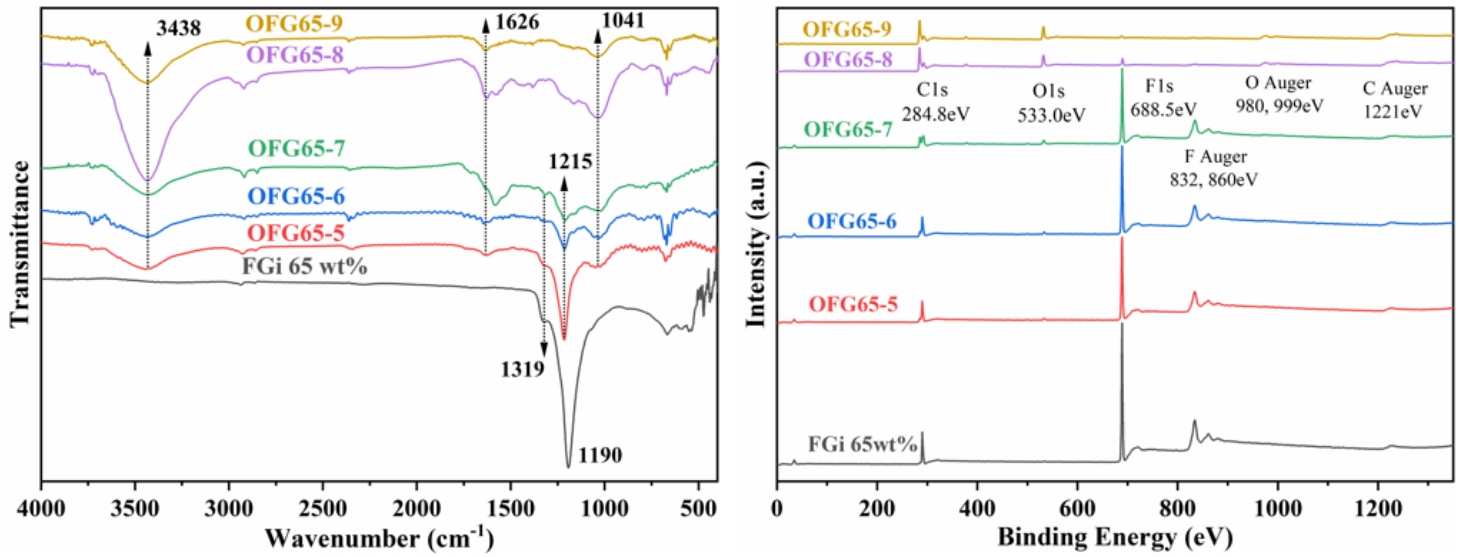

(a) FT-IR spectrum (b) XPS spectrum

Figure 8

(a) FT-IR and (b) XPS spectra of OFG65-5(20℃), OFG65-6(40℃), OFG65-7(60℃), OFG65-8(80℃) and OFG65-9(100℃)

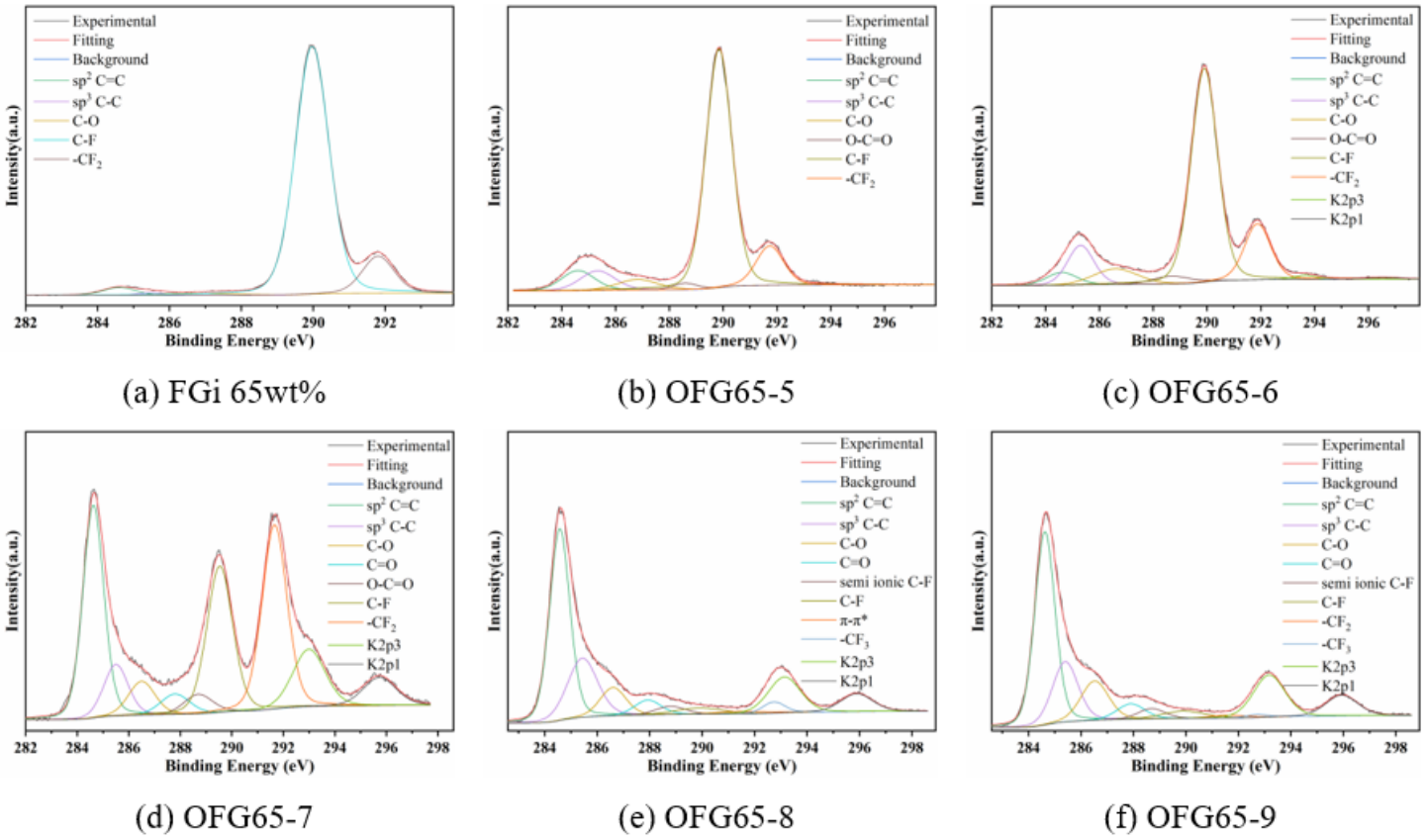

Figure 9

High-resolution C1s spectra of OFG65 after KOH heating method

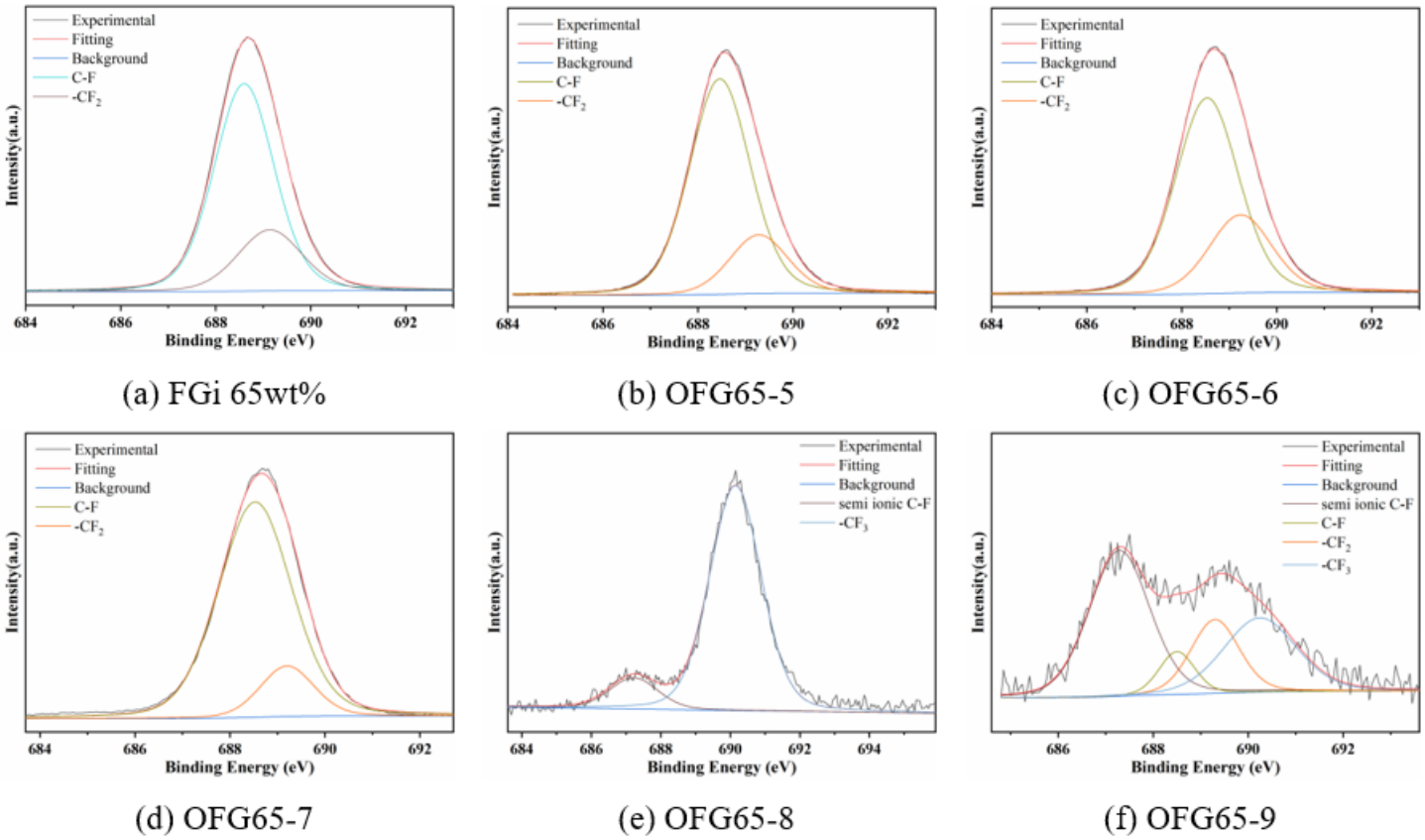

Figure 10

High-resolution F1s spectra of OFG65 after KOH heating method

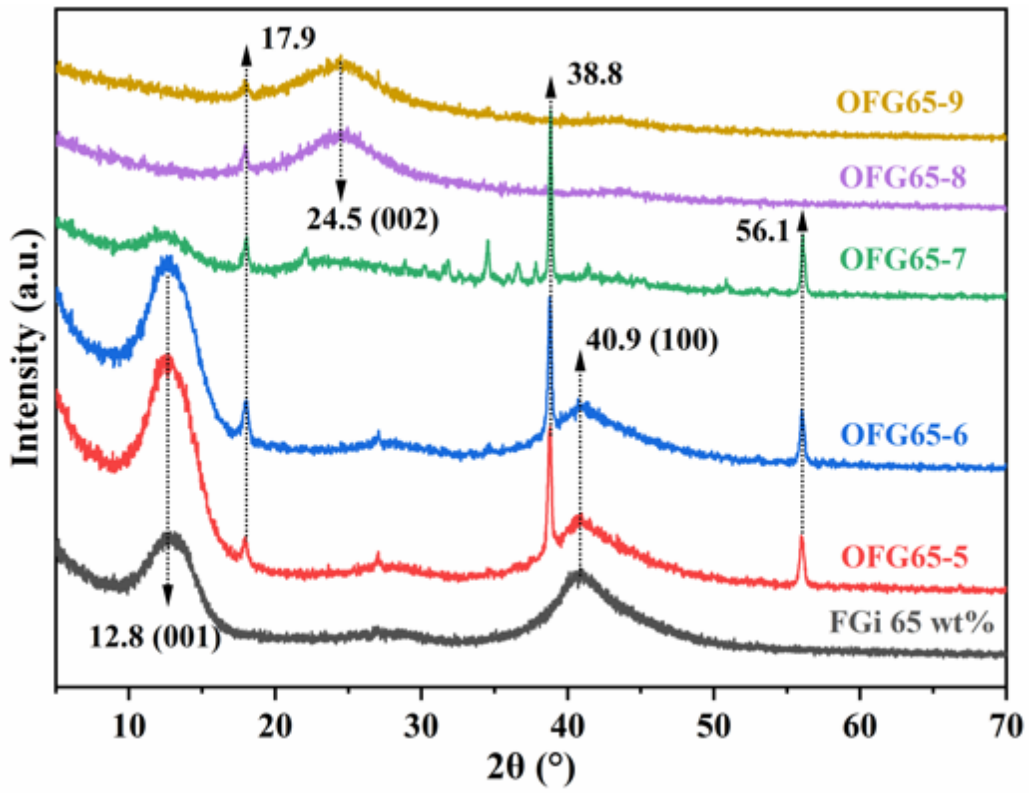

Figure 11

XRD spectrum of OFG65 after KOH heating methods

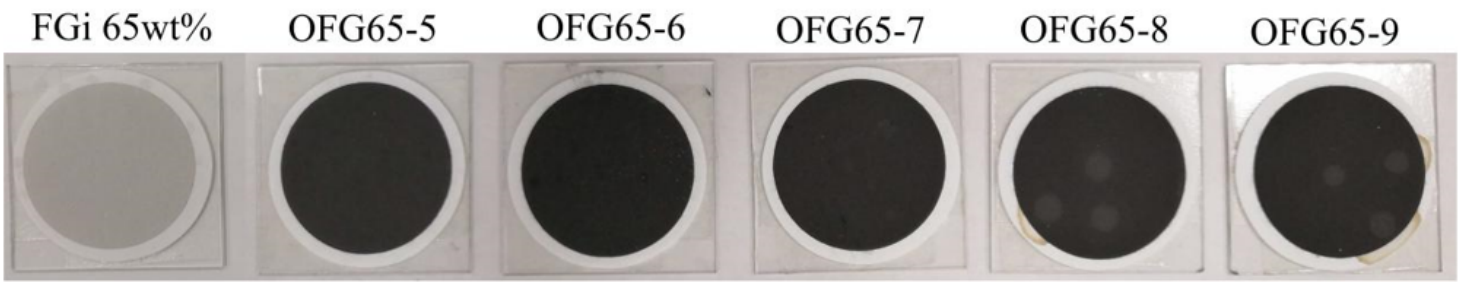

Figure 12

Photos of OFG65 after KOH heating methods

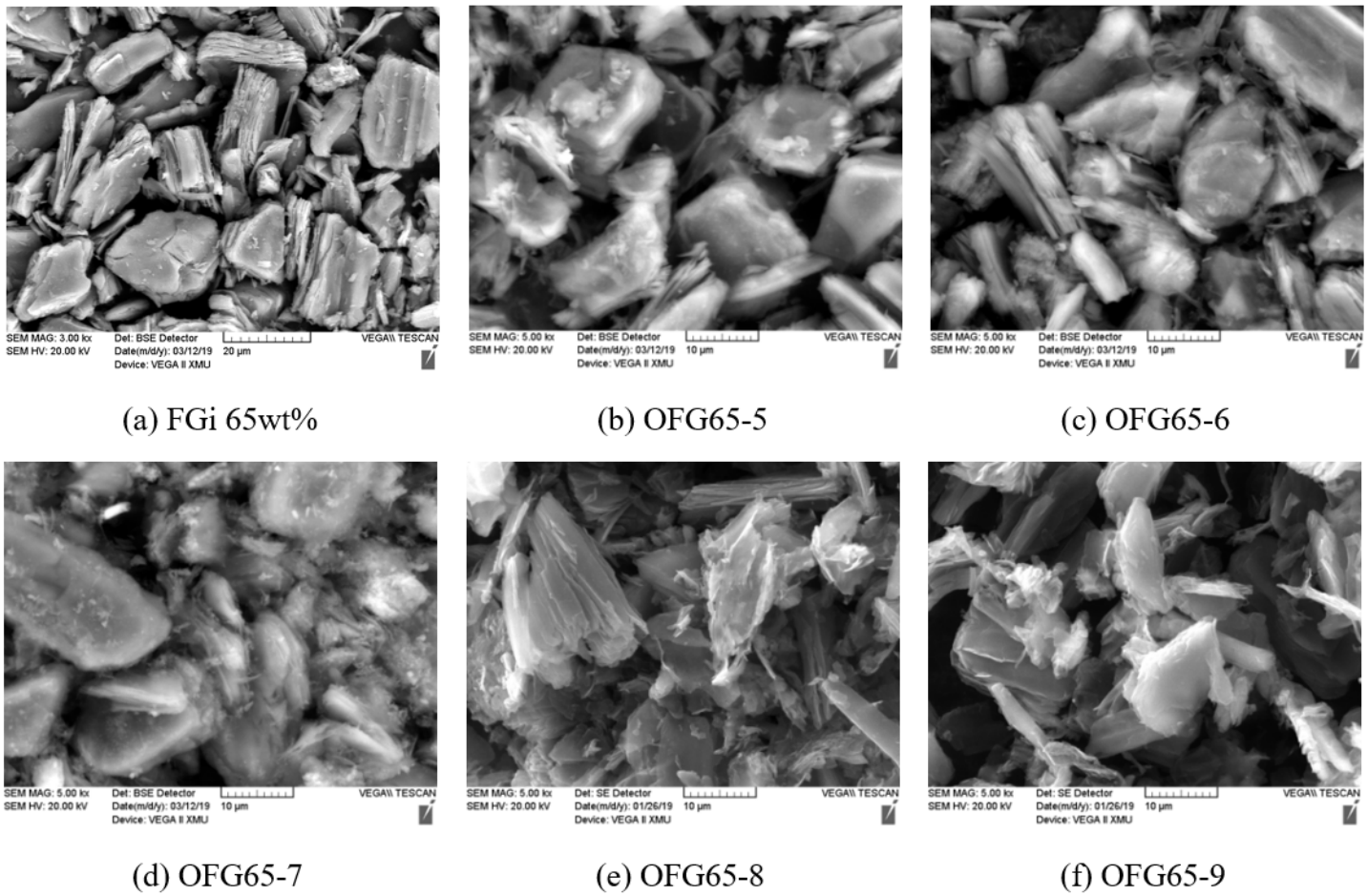

Figure 13

SEM images of OFG65 after KOH heating methods

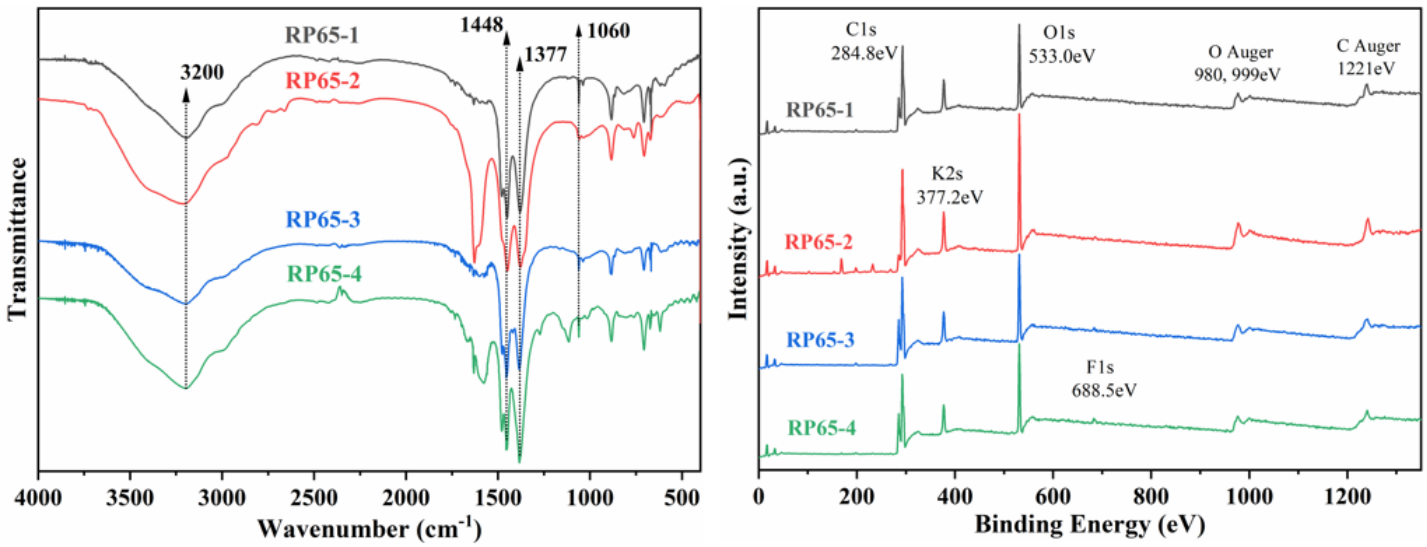

(a) FT-IR spectrum (b) XPS spectrum

Figure 14

(a) FT-IR and (b) XPS spectra of residual products of KOH electrochemical reaction

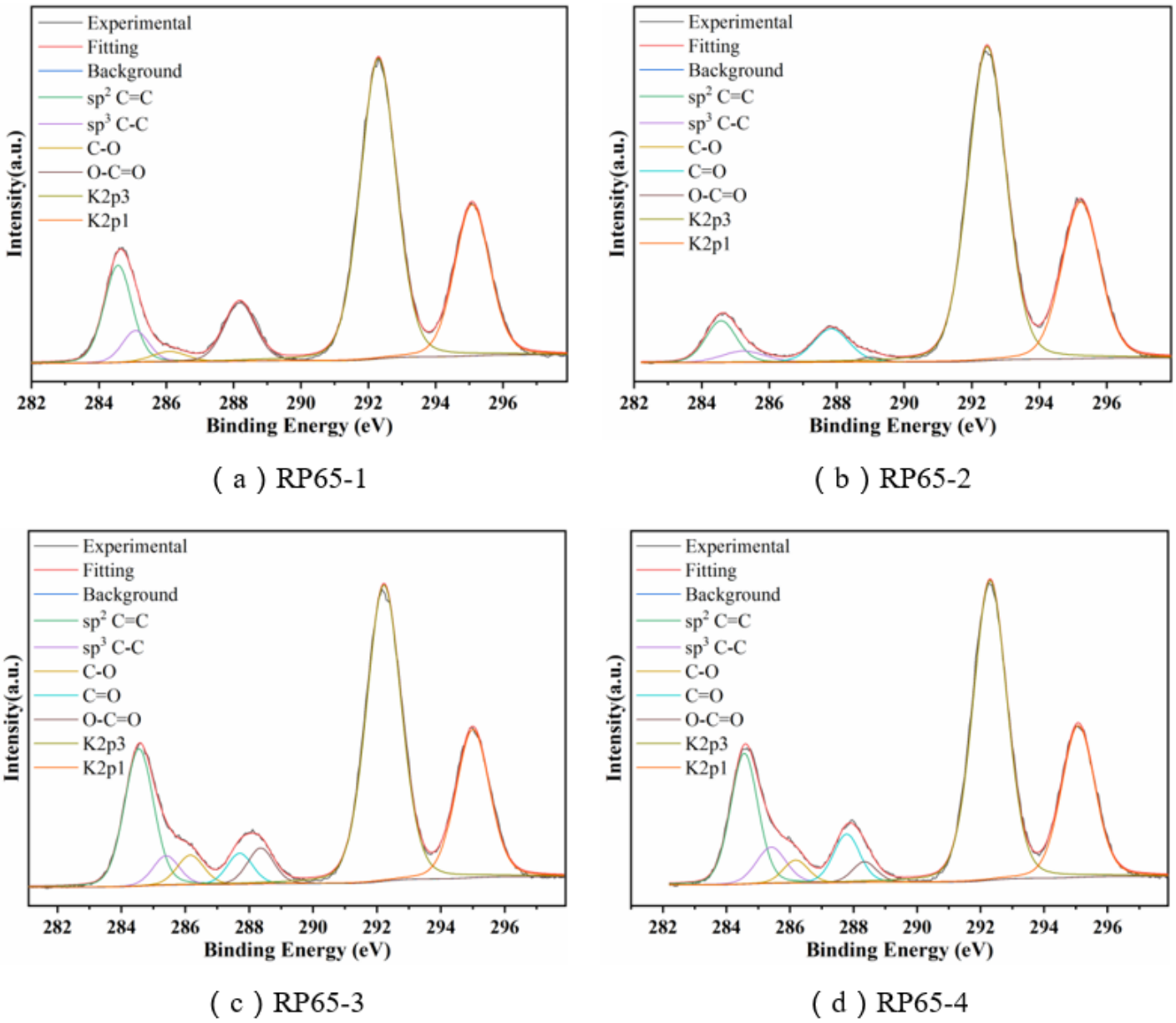

Figure 15

High-resolution C1s spectra of residual products of KOH electrochemical reaction

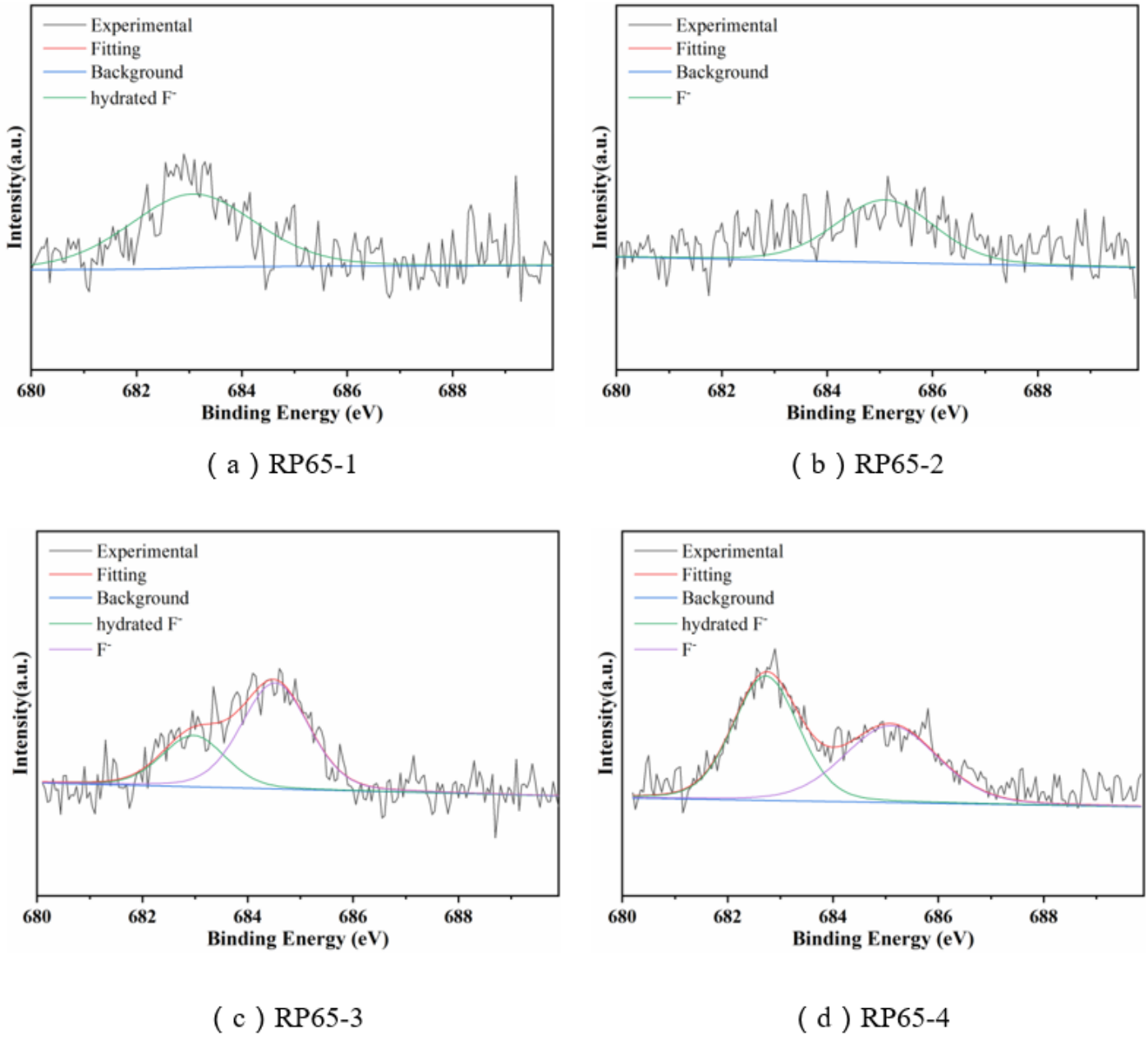

Figure 16

High-resolution F1s spectra of residual products of KOH electrochemical reaction

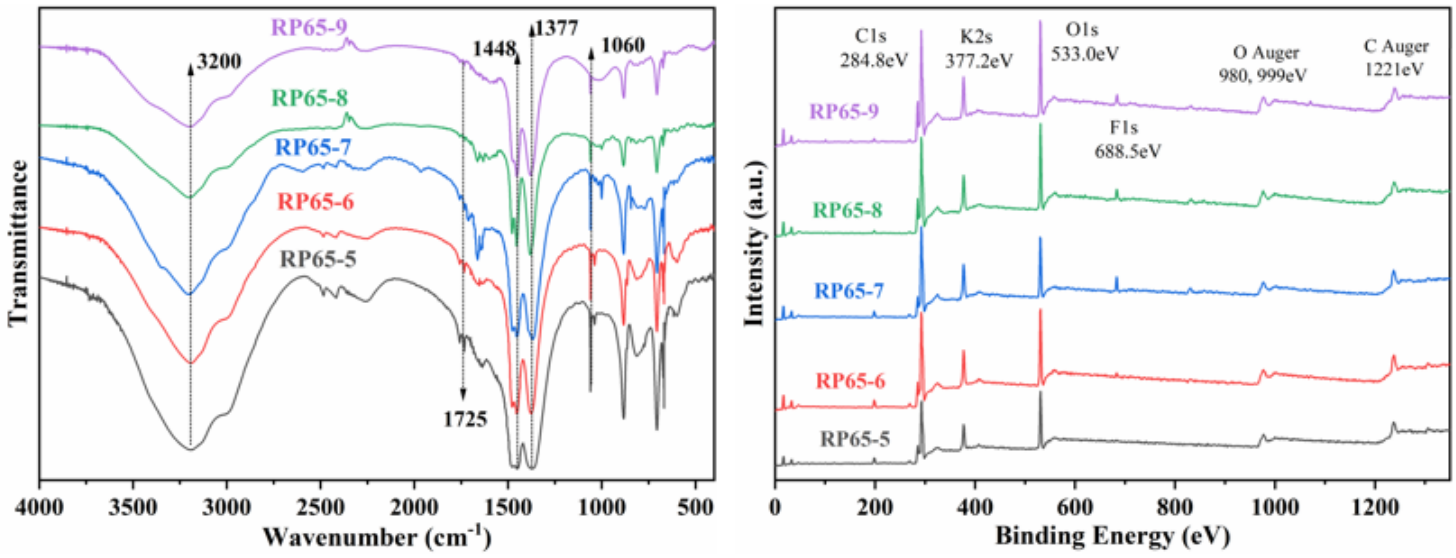

(a) FT-IR spectrum (b) XPS spectrum

Figure 17

(a) FT-IR and (b) XPS spectra of residual products of KOH heating reaction

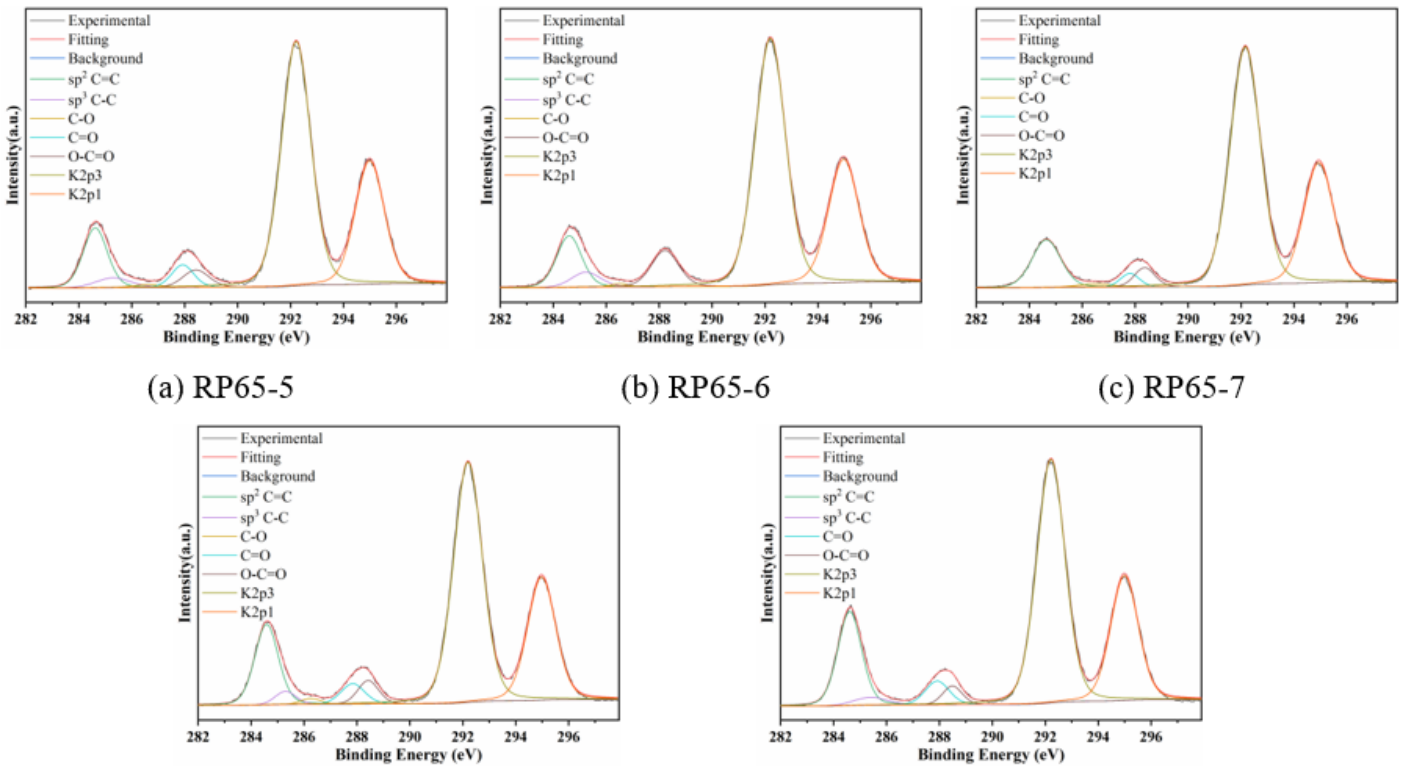

(a) RP65-5 (b) RP65-6 (c) RP65-7

(d) RP65-8 (e) RP65-9

Figure 18

High-resolution C1s spectra of residual products of KOH heating reaction

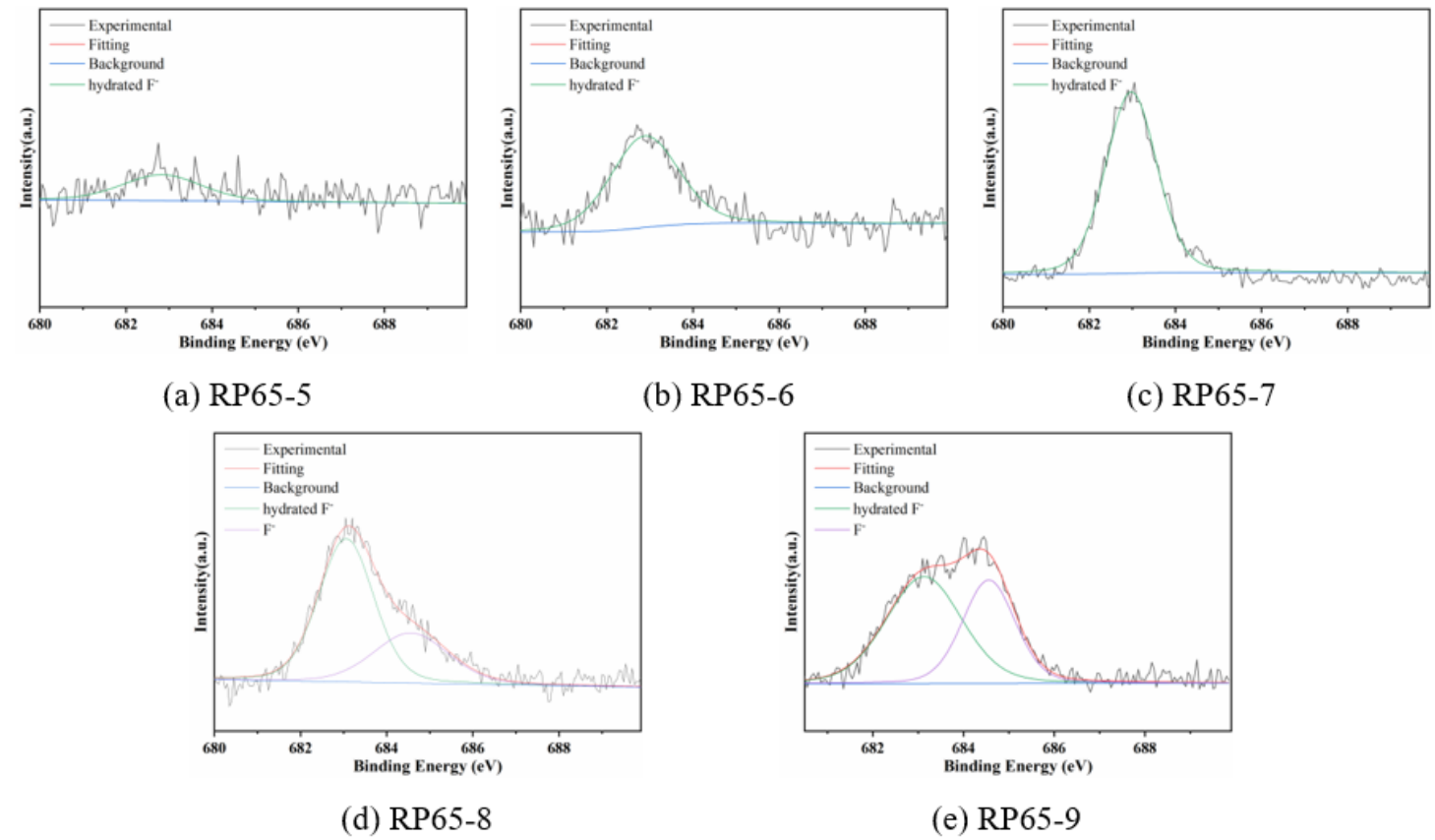

Figure 19

High-resolution F1s spectra of residual products of KOH heating reaction

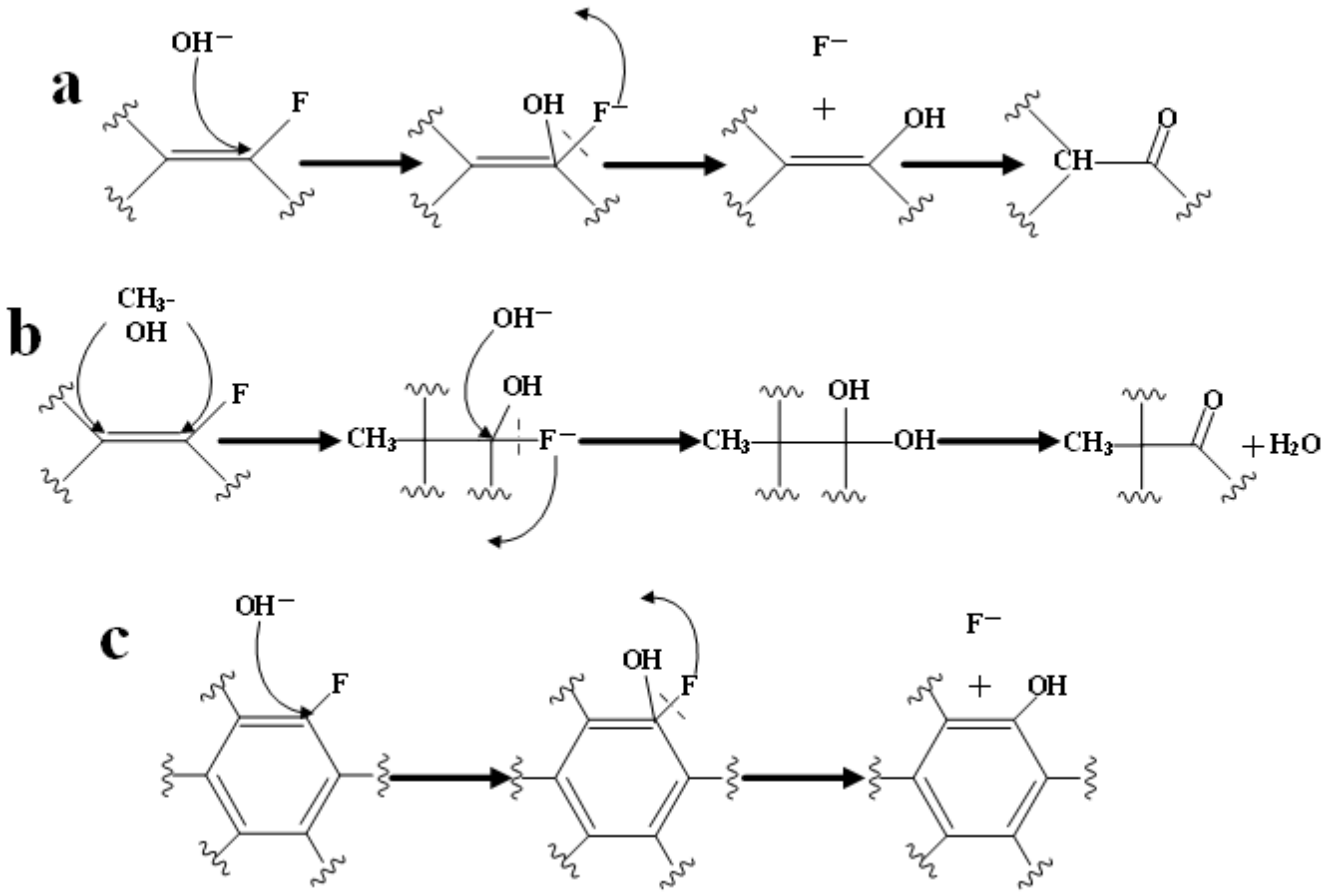

Figure 20

Nucleophilic reaction mechanism between KOH and C-F bond

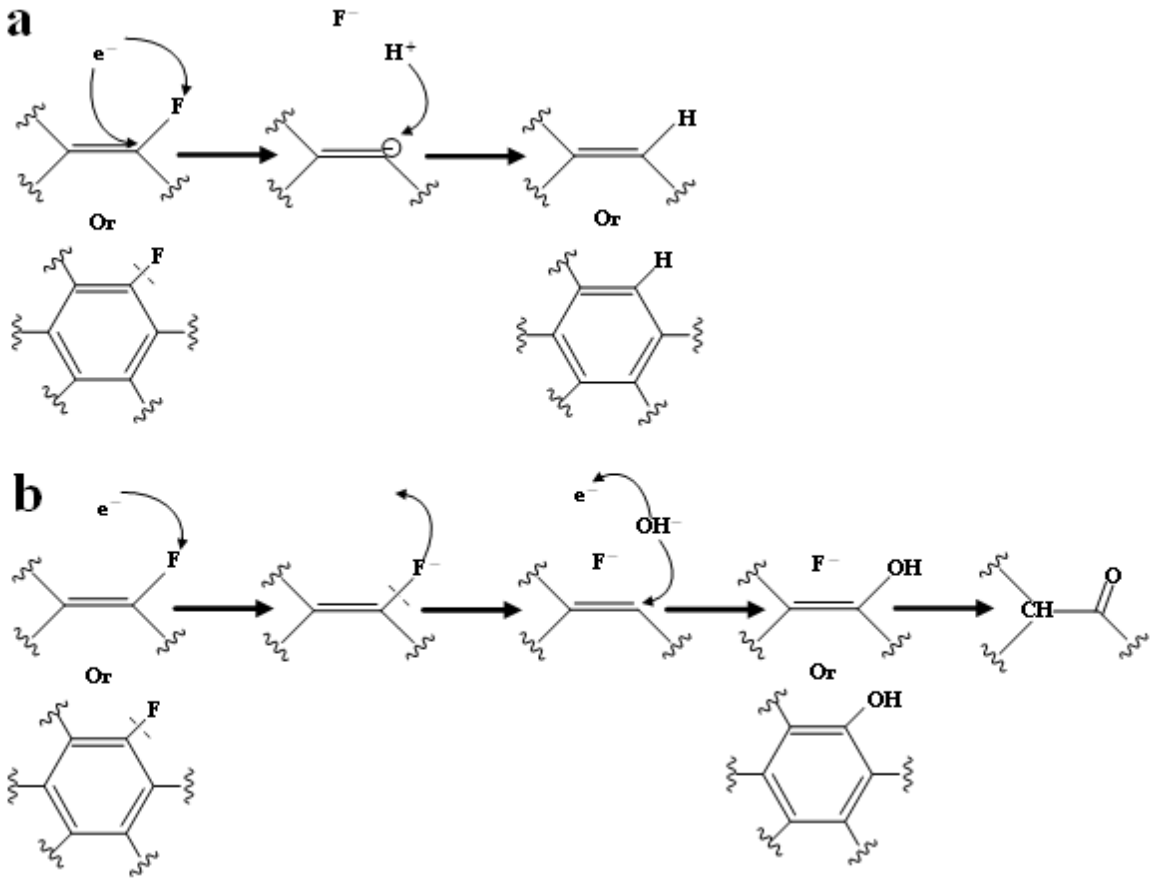

Figure 21

Nucleophilic reaction mechanism under electron transfer condition

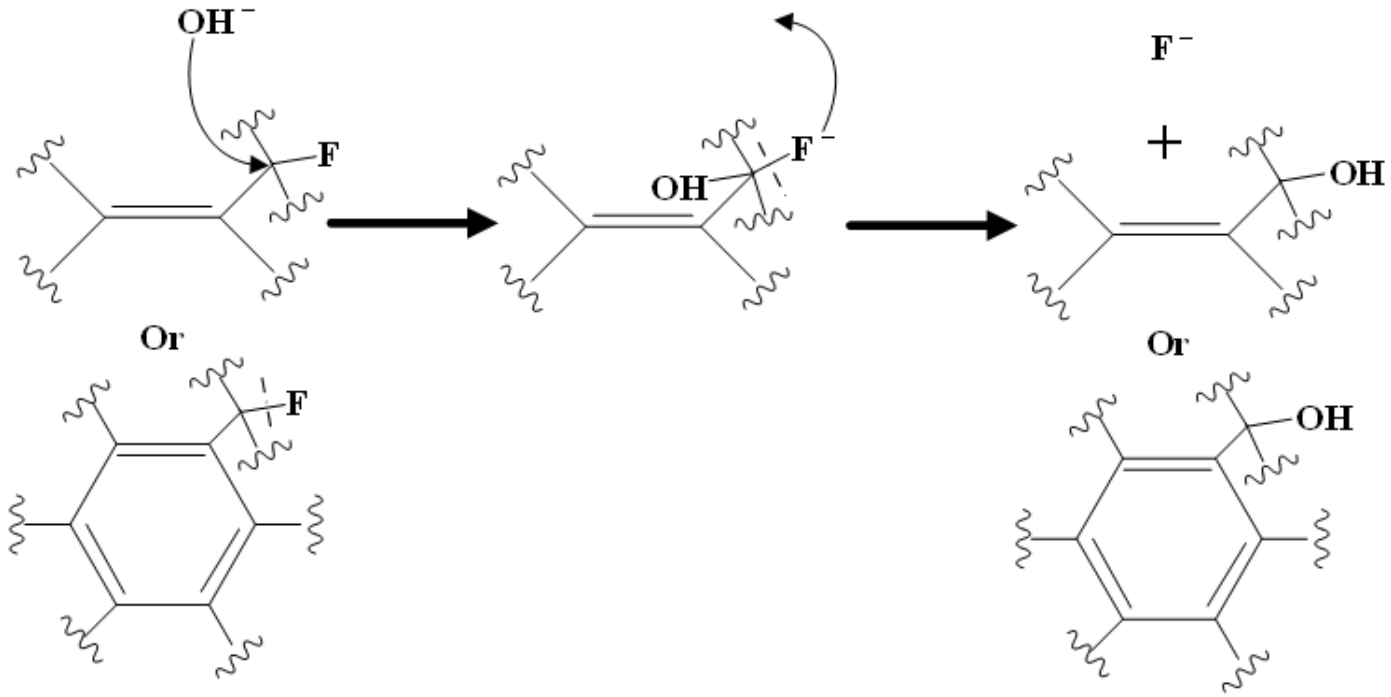

Figure 22

Nucleophilic reaction mechanism between KOH and subactive C-F bond

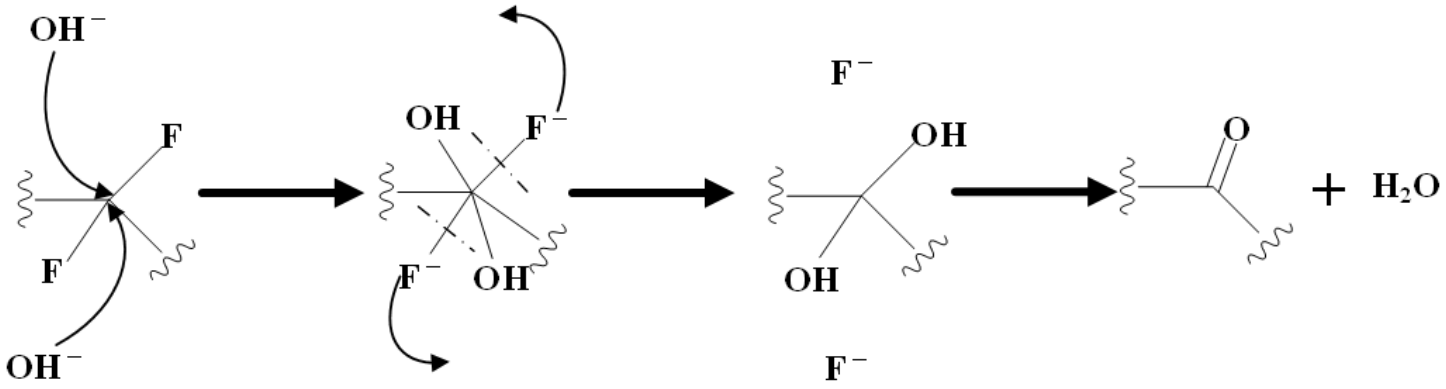

Figure 23

Carbonyl formation mechanism in OFG65 products

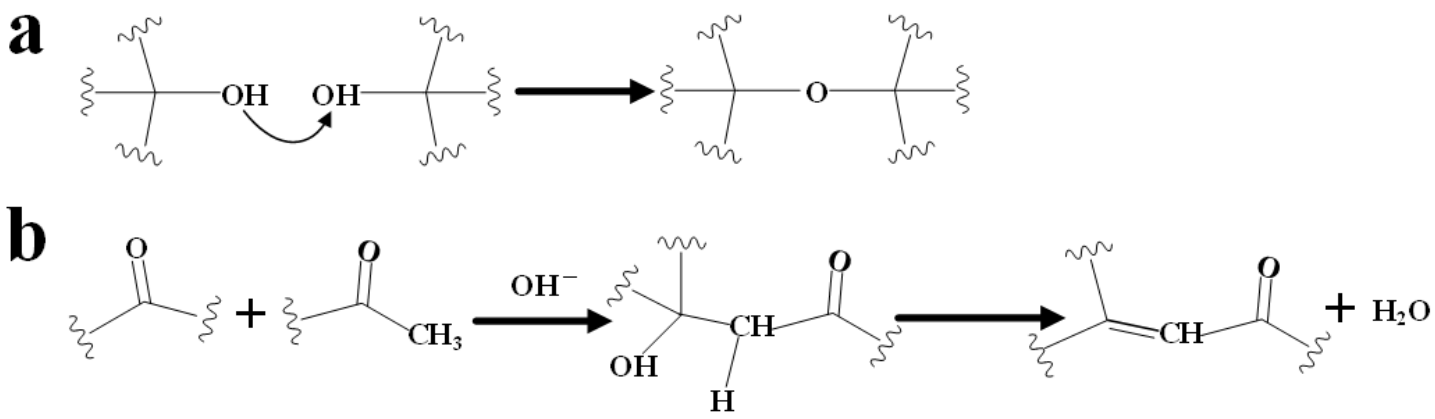

Figure 24

OFG deoxidation mechanism under strong alkalinity

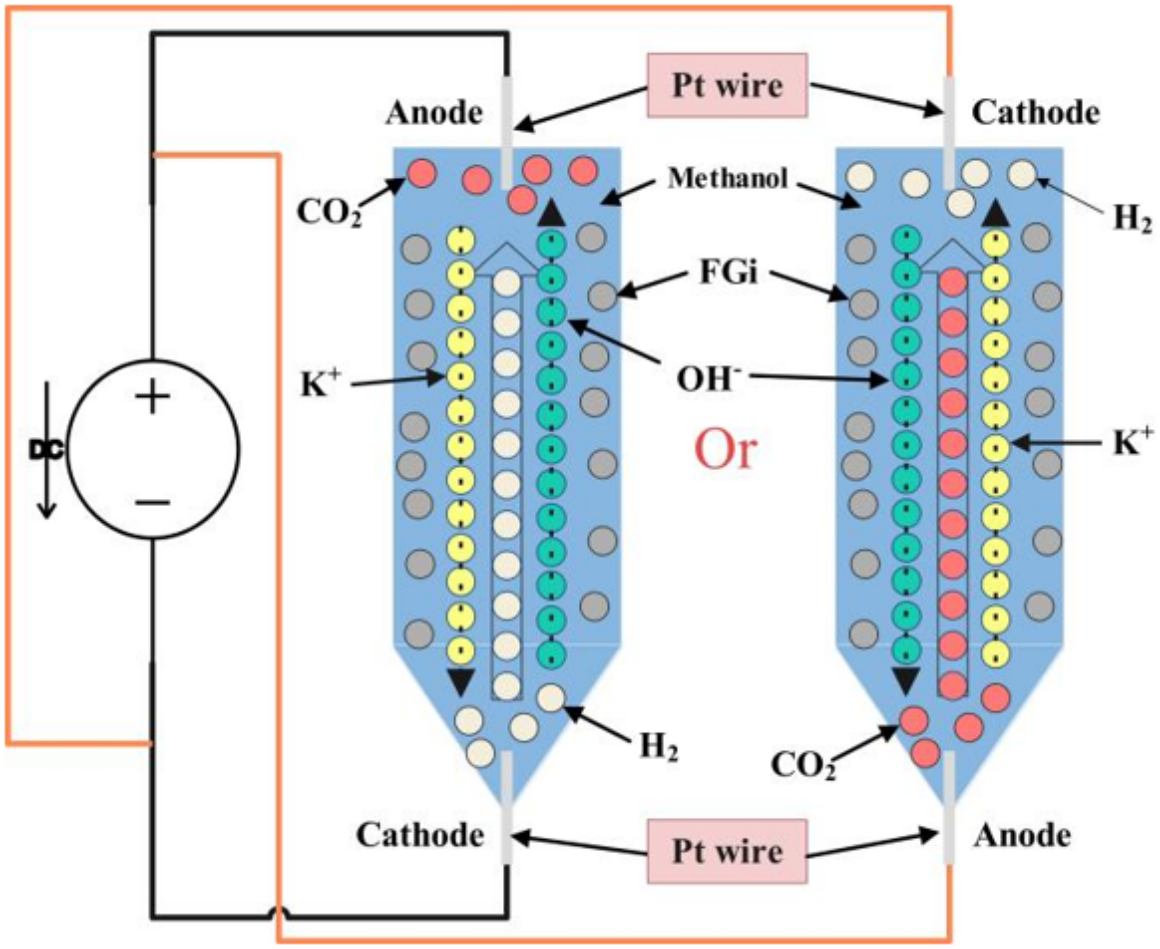

Figure 25

Principle display of the electrolysis of KOH methanol solution

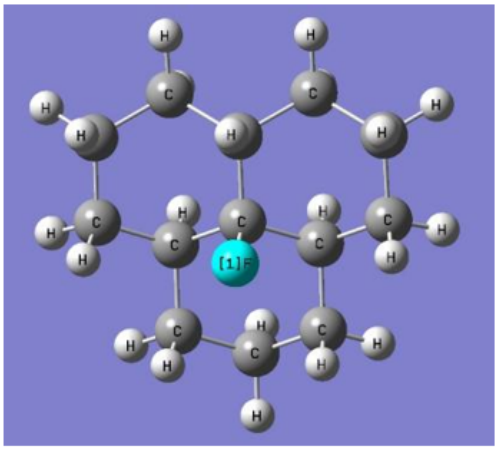

(a) Isolated carbon-fluorine bond

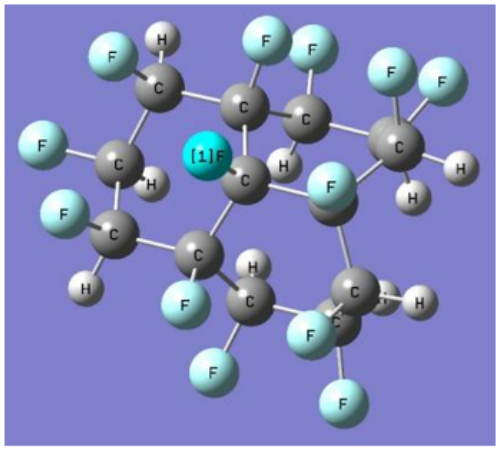

(b) Carbon-fluorine bond surrounding F atoms

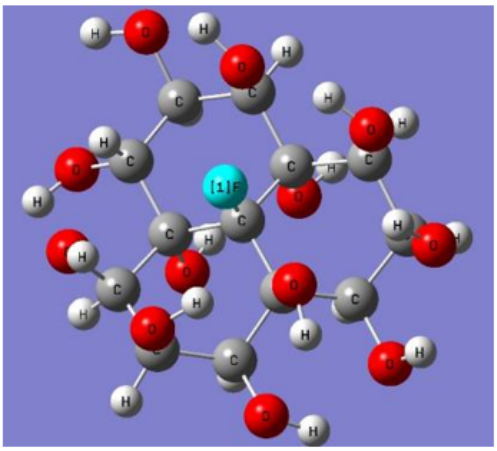

(c) C-F bond surrounding hydroxyl groups

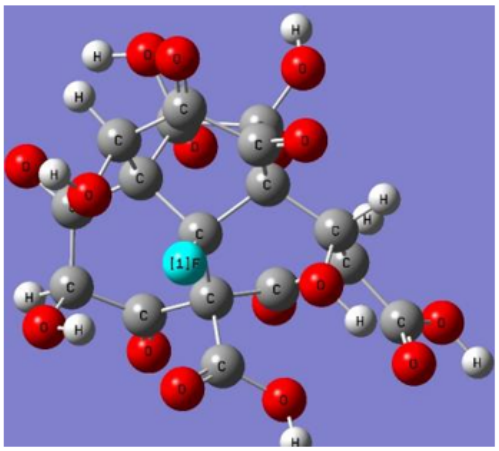

(d) C-F bond surrounding oxygen-containing groups

Figure 26

Schematic structure of the carbon fluorine bond at different positions

Supplementary Files

This is a list of supplementary files associated with this preprint. Click to download.

- supplymentmaterial20220105.docx